

# Old World Arenavirus Infection Interferes with the Expression of Functional $\alpha$ -Dystroglycan in the Host Cell<sup>□</sup>

Jillian M. Rojek,\* Kevin P. Campbell,<sup>†</sup> Michael B.A. Oldstone,\* and Stefan Kunz\*

\*Viral Immunobiology Laboratory, Molecular and Integrative Neurosciences Department, The Scripps Research Institute, La Jolla, CA 92037; and <sup>†</sup>Departments of Molecular Physiology and Biophysics, Neurology, and Internal Medicine, Howard Hughes Medical Institute, University of Iowa College of Medicine, Iowa City, IA 52242

Submitted April 25, 2007; Revised August 2, 2007; Accepted August 22, 2007  
Monitoring Editor: Jean Schwarzbauer

**$\alpha$ -Dystroglycan ( $\alpha$ -DG) is an important cellular receptor for extracellular matrix (ECM) proteins as well as the Old World arenaviruses lymphocytic choriomeningitis virus (LCMV) and the human pathogenic Lassa fever virus (LFV). Specific O-glycosylation of  $\alpha$ -DG is critical for its function as receptor for ECM proteins and arenaviruses. Here, we investigated the impact of arenavirus infection on  $\alpha$ -DG expression. Infection with an immunosuppressive LCMV isolate caused a marked reduction in expression of functional  $\alpha$ -DG without affecting biosynthesis of DG core protein or global cell surface glycoprotein expression. The effect was caused by the viral glycoprotein (GP), and it critically depended on  $\alpha$ -DG binding affinity and GP maturation. An equivalent effect was observed with LFVGP. Viral GP was found to associate with a complex between DG and the glycosyltransferase LARGE in the Golgi. Overexpression of LARGE restored functional  $\alpha$ -DG expression in infected cells. We provide evidence that virus-induced down-modulation of functional  $\alpha$ -DG perturbs DG-mediated assembly of laminin at the cell surface, affecting normal cell–matrix interactions.**

## INTRODUCTION

The interaction of a virus with its cellular receptor(s) is the first step in every viral infection and a key determinant for the host-range, tissue tropism, and disease potential of a virus. Although the primary role of virus receptors is to bind and thus concentrate virus particles on the cell surface, there is increasing evidence that virus binding can also affect receptor function, facilitating viral entry and replication (Smith and Helenius, 2004; Coyne and Bergelson, 2006; Marsh and Helenius, 2006; Helenius, 2007). Furthermore, some viruses have evolved mechanisms to modulate the biosynthesis and cellular trafficking of their receptors during their life cycles. Such virus-induced changes in receptor expression may not only be crucial for optimal virus multiplication but also may affect normal host cell function. This makes viruses powerful probes to investigate the cell biology of their receptor molecules.

Arenaviruses are noncytolytic RNA viruses that merit significant attention as powerful experimental models and important human pathogens. Studies on the infection of the prototypic arenavirus lymphocytic choriomeningitis virus (LCMV) in its natural host, the mouse, provided fundamental concepts in virology and immunology (Oldstone, 2002).

Lassa fever virus (LFV) causes a severe hemorrhagic fever in humans with >300,000 infections and several thousand deaths per year (McCormick and Fisher-Hoch, 2002; Geisbert and Jahrling, 2004). The genome of arenaviruses consists of two single-stranded RNA species, a large segment encoding the virus polymerase (L) and a small zinc finger motif protein (Z), and a small segment encoding the virus nucleoprotein (NP) and glycoprotein precursor (GPC) (Buchmeier *et al.*, 2007). GPC is processed into GP1, implicated in receptor binding, and the transmembrane GP2, which is structurally similar to the fusion active portions of other viral GPs.

The cellular receptor of LCMV, LFV, and Clade C New World arenaviruses is  $\alpha$ -dystroglycan ( $\alpha$ -DG), an important cell surface receptor for extracellular matrix (ECM) proteins (Cao *et al.*, 1998; Spiropoulou *et al.*, 2002). Encoded as a single protein, DG is cleaved into the extracellular  $\alpha$ -DG, and membrane anchored  $\beta$ -DG (Barresi and Campbell, 2006).  $\alpha$ -DG has a central, highly glycosylated mucin-type domain that connects the globular N- and C-terminal domains. At the extracellular site,  $\alpha$ -DG undergoes high-affinity interactions with the ECM proteins laminin, agrin, perlecan, and neurexins.  $\alpha$ -DG is noncovalently associated with  $\beta$ -DG, which binds intracellularly to the cytoskeletal adaptor proteins dystrophin and utrophin, and signaling molecules. DG is expressed in most developing and adult tissues, typically in cell types that adjoin basement membranes (Durbeej *et al.*, 1998). At those sites, DG provides a molecular link between the ECM and the actin-based cytoskeleton, and it is crucial for normal cell–matrix interactions (Henry and Campbell, 1998; Henry *et al.*, 2001).

In mammals,  $\alpha$ -DG is subject to complex O-glycosylation that is crucial for its function as a receptor for ECM proteins (Barresi and Campbell, 2006). These modifications involve known and putative glycosyltransferases, including the pro-

This article was published online ahead of print in *MBC in Press* (<http://www.molbiolcell.org/cgi/doi/10.1091/mbc.E07-04-0374>) on August 29, 2007.

<sup>□</sup> The online version of this article contains supplemental material at *MBC Online* (<http://www.molbiolcell.org>).

Address correspondence to: Stefan Kunz ([stefankunz@scripps.edu](mailto:stefankunz@scripps.edu)).

Abbreviations used: DG, dystroglycan; ECM, extracellular matrix; LCMV, lymphocytic choriomeningitis virus; LFV, Lassa virus; MOI, multiplicity of infection.

tein *O*-mannosyltransferases POMT1 and POMT2, protein *O*-mannose  $\beta$ 1,2-*N*-GlcNAc transferase 1 (POMGnT1), LARGE, fukutin, and fukutin-related protein (FKRP). The genes implicated in  $\alpha$ -DG glycosylation are targeted in a number of congenital muscular dystrophies called “dystroglycanopathies” that are caused primarily by aberrant glycosylation of  $\alpha$ -DG and its loss of function as an ECM receptor (Cohn, 2005; Barresi and Campbell, 2006; Kanagawa and Toda, 2006). POMT1/2 and POMGnT1 are involved in the biosynthesis of the unusual *O*-mannosyl oligosaccharide SiaA $\alpha$ 2-3Gal $\beta$ 1-4GlcNAc $\beta$ 1-2Man, which is found in high abundance on  $\alpha$ -DG (Yoshida *et al.*, 2001; Many *et al.*, 2004). Another crucial glycan modification of  $\alpha$ -DG involves the putative glycosyltransferases LARGE and LARGE2, which localize in the Golgi and are implicated in the biosynthesis of a glycan polymer of unknown structure (Barresi *et al.*, 2004; Kanagawa *et al.*, 2004; Barresi and Campbell, 2006; Kanagawa and Toda, 2006). Modification of the N-terminal part of the mucin-like domain of  $\alpha$ -DG by LARGE is essential for its function as an ECM receptor (Kanagawa *et al.*, 2004). Recognition by LARGE involves the N-terminal domain of  $\alpha$ -DG, which is subsequently cleaved by a convertase-like activity. Interestingly, LARGE can functionally bypass defects in other enzymes involved in the functional glycosylation of  $\alpha$ -DG, indicating a key role in the functional glycosylation of the receptor (Barresi *et al.*, 2004; Patnaik and Stanley, 2005). Recent studies reported also a critical role for protein *O*-mannosylation and LARGE-dependent modification for the function of  $\alpha$ -DG as a receptor for Old World and Clade C New World arenaviruses, indicating similarity in receptor recognition between ECM proteins and arenaviruses (Imperiali *et al.*, 2005; Kunz *et al.*, 2005a; Rojek *et al.*, 2007).

Our present study investigated the impact of arenavirus infection on the expression of functional  $\alpha$ -DG in the host cell. Infection of cells with an immunosuppressive LCMV isolate caused a marked reduction in the expression of functional  $\alpha$ -DG without affecting the biosynthesis of the DG core protein or global cell surface glycoprotein expression. The effect was caused by the viral GP, critically depended on high  $\alpha$ -DG binding affinity, and it required proper GP maturation. The viral GP was found to associate with DG and LARGE in the Golgi, and overexpression of LARGE restored expression of functional  $\alpha$ -DG in infected cells. In the host cell, virus-induced interference with functional  $\alpha$ -DG expression perturbed DG-mediated assembly of laminin, affecting normal cell–matrix interaction and cell function.

## MATERIALS AND METHODS

### Proteins and Antibodies

Natural mouse laminin-1 and human fibronectin were obtained from Invitrogen (Carlsbad, CA). Monoclonal antibodies (mAbs) 83.6 (mouse IgG2a anti-LCMVGP2) and 113 (anti-LCMVNP) have been described previously (Buchmeier *et al.*, 1981; Weber and Buchmeier, 1988) as have mAb BE08 anti-Junin GP1 (Sanchez *et al.*, 1989), mAb IIH6 anti- $\alpha$ -DG (mouse IgM), polyclonal antibody AP83 to  $\beta$ -DG (Ervasti and Campbell, 1993), and polyclonal antibody GT20ADG anti- $\alpha$ -DG core protein (Kanagawa *et al.*, 2004). mAb 8C5 anti- $\beta$ -DG was from Novocastra (Newcastle, United Kingdom). Other mAbs included mouse anti- $\alpha$ -tubulin (Sigma-Aldrich; St. Louis, MO), mouse anti-HA F-7 (Santa Cruz Biotechnology, Santa Cruz, CA), mouse anti-FLAG M2 (Sigma-Aldrich, St. Louis, MO), mouse mAb (IgG1) anti-endoplasmic reticulum (ER) calnexin (BD Biosciences, San Jose, CA), and mouse mAb (IgG1) anti-GM-130 (BD Biosciences). Mouse anti-FLAG M2 coupled to agarose was purchased from Sigma-Aldrich. Primary polyclonal antibodies (pAb) included rabbit anti-laminin-1 IgG from Sigma-Aldrich, rabbit anti-hemagglutinin (HA) IgG Y-11 (Santa Cruz Biotechnology), and rabbit anti-myc IgG A-14 (Santa Cruz Biotechnology), and rabbit (Santa Cruz Biotechnology) and goat (Abcam, Cambridge, MA) anti-flag IgG. Purified R-phycoerythrin (R-PE)-conjugated mAbs to human  $\beta$ 1 integrin,  $\alpha$ 1 integrin,  $\alpha$ 2 integrin,  $\alpha$ 3

integrin,  $\alpha$ 6 integrin, transferrin receptor, and major histocompatibility complex (MHC) class I (HLA-A, -B, and -C) were from BD Biosciences Pharmingen (San Diego, CA). R-PE-conjugated anti-mouse IgM and IgG, rhodamine-X-conjugated anti-mouse and rabbit IgG, and fluorescein isothiocyanate (FITC)-conjugated anti-mouse, anti-rabbit, and anti-goat IgG, biotin anti-mouse IgG, and Streptavidin-Cy5 were from Jackson ImmunoResearch Laboratories (West Grove, PA). Anti-mouse, anti-rabbit, anti-goat, anti-human IgG horseradish peroxidase (HRP)-conjugated were obtained from Pierce Chemical (Rockford, IL).

### Expression Constructs

The following expression constructs have been described previously: pC-LCMVGP, expressing LCMVGP derived from ARM53b and cl-13 (Kunz *et al.*, 2003a); pC-LCMVNP, expressing LCMVNP (Lee *et al.*, 2000); a pGEM vector expressing LCMV HA-tagged LCMV polymerase (Sanchez and de la Torre, 2005); pC-ZHA, expressing HA-tagged LCMV matrix protein (Perez *et al.*, 2003); pC-LFVGP, expressing the GP of LFV strain Josiah (Kunz *et al.*, 2005a); pC-JuninGP, expressing the GP of Junin strain XJ13 (Rojek *et al.*, 2006); and pDNA3 vector expressing CD46-EGFP fusion protein (Kunz *et al.*, 2003b). For construction of the C-terminally flag-tagged variants of LFVGP, LCMVGP cl-13, and Junin GP, the C-terminally myc-tagged LARGE, N-terminally HA-tagged DG (HADG), and C-terminally HA-tagged DG (DGHA), see Supplemental Material.

### Cells and Cell Lines

African green monkey kidney (Vero-E6), human embryonic kidney (HEK)293, and A549 human lung carcinoma cells (ATCC CCL-185) were maintained in DMEM containing 10% fetal calf serum and supplemented with glutamine, and penicillin/streptomycin. Wild-type [DG (+/+)], hemizygous [DG (+/-)], and DG-deficient [DG (-/-)] embryonic stem (ES) cells were maintained as described previously (Henry and Campbell, 1998).

### Viruses, Purification, and Quantification

The recombinant adenovirus (AdV) Ad5/LARGE-EGFP and Ad5/EGFP have been described previously (Barresi *et al.*, 2004), as have AdV vectors expressing wild-type DG, and the mutants DGE (DG $\Delta$ 30-316) and DGF (DG $\Delta$ 317-408) (Kunz *et al.*, 2001). Seed stocks of LCMV and Pichinde were prepared by growth in BHK-21 cells. Origin, passage, and characteristics of LCMV ARM53b and clone-13 have been described previously (Dutko and Oldstone, 1983; Ahmed *et al.*, 1984). Purified Pichinde virus stocks were produced and titers determined as described previously (Dutko and Oldstone, 1983).

### Virus Infection of Cells

Infections of Vero, 293T, A549, and mouse ES cells with LCMV and/or adenoviruses were carried out in either eight-well LabTek chamber slides (Nalge Nunc International, Rochester, NY) at  $2 \times 10^4$  cells/well or six-well trays at  $5 \times 10^5$  cells/well, precoated with PLL for 293T cells and 10  $\mu$ g/ml fibronectin for ES cells. Seed stocks of LCMV cl13 ( $1 \times 10^8$  plaque-forming units/ml) were diluted to various multiplicities of infection (MOIs) and added to cells for 1 h at 37°C. Virus mix was removed, cells washed twice with medium, and incubated for 48 h. For rescue experiments, adenoviruses (Ad5/LARGE and Ad5/LacZ as a control) were added to cells at an MOI of 100 and incubated for 4 h at 37°C, washed twice with medium, and then cultured for the time periods indicated. Infection of mouse ES cells with AdV vectors expressing wild-type DG, DGE, and DGF was performed as described previously (Kunz *et al.*, 2001).

### Expression of Recombinant Proteins

For transfection with SuperFect (QIAGEN, Valencia, CA), 293T cells were plated  $\sim 8 \times 10^5$  cells/well in six-well trays precoated with 100  $\mu$ g/ml poly-L-lysine. In total, 2  $\mu$ g of total expression plasmid DNA was mixed with 125  $\mu$ l of reduced serum medium, Opti-MEM (Invitrogen), and vortexed. Then, 12  $\mu$ l of SuperFect reagent was added and incubated for 10 min at room temperature. Next, 500  $\mu$ l of 293T cell medium was added to the mixture, the medium was removed from the cells, and the mix was added to the cells for 3 h at 37°C. After incubation, the transfection mix was removed from the cells, and 4 ml/well warm medium was added and incubated for 48 h under the same conditions. Transfection efficiencies as determined by immunofluorescence detection of transgenes were  $>90\%$ .

For transfection of mouse ES cells, the Mouse ES Cell Nucleofector kit from Amaxa Biosystems (Gaithersburg, MD) was used according to the manufacturer's recommendation (<http://www.amaxa.com>). For assessment of transfection efficiency,  $5 \times 10^6$  cells were transfected with 10  $\mu$ g of an enhanced green fluorescent protein (EGFP)-expressing control plasmid using Nucleofector program A-013, and cells were examined after 48 h by direct fluorescence microscopy. In all mouse ES cell lines tested, transfection efficiencies were consistently  $>80\%$ .

### Immunoblotting and Laminin Overlay Assay

Standard immunoblotting involved proteins being separated by SDS-polyacrylamide gel electrophoresis (PAGE) and transferred to nitrocellulose. After blocking in 5% (wt/vol) skim milk in PBS, membranes were incubated with 10  $\mu$ g/ml primary antibody anti-human IgG Fc, mouse mAb IIH6, sheep/goat core  $\alpha$ -DG, mouse mAb to  $\beta$ -DG, mouse mAb to  $\alpha$ -tubulin, mAb anti-LCMV-GP2 (83.6), rabbit pAb anti-myc A-14, mouse mAb anti-HA F-7, or rabbit anti-HA Y11 in 2% (wt/vol) skim milk, phosphate-buffered saline (PBS) overnight at 6°C. After several washes in PBS, 0.1% (wt/vol) Tween 20 (PBST), secondary antibodies coupled to HRP were applied 1:5000 in PBST for 1 h at room temperature. Blots were developed by enhanced chemiluminescence (ECL) by using SuperSignal West Pico ECL Substrate (Pierce Chemical). Laminin overlay assay (LOA) was performed as described previously (Michele *et al.*, 2002).

### Flow Cytometry

For cell surface stainings, cells were detached with enzyme-free cell dissociation solution (Sigma-Aldrich), resuspended in fluorescence-activated cell sorting (FACS) buffer (1%, vol/vol fetal bovine serum [FBS], 0.1%, wt/vol sodium azide, and PBS), and plated in conical 96-well trays. For cell surface staining of functionally glycosylated  $\alpha$ -DG, cells were incubated with mAb IIH6 (1:145), for staining of the  $\alpha$ -DG core protein, antibody GT20ADG was applied at 1:50 dilution, and for staining of viral GP, cells were incubated with mAb 83.6 (1:50). Incubation was for 1 h on ice in FACS buffer. Cells were then washed twice in FACS buffer and labeled with PE-conjugated secondary antibodies (1:100 in FACS buffer) for 45 min on ice in the dark. After two wash-steps in 1% (vol/vol) FBS in PBS, cells were fixed with 4% (wt/vol) paraformaldehyde, PBS for 10 min at room temperature in the dark. The cells were washed twice with PBS, and then they were analyzed with a FACSCalibur flow cytometer (BD Biosciences, San Jose CA) using Cell Quest software. Image analysis was done using FloJo software (Tree Star, Ashland, OR).

### RNA Analysis by Reverse Transcription-Polymerase Chain Reaction (RT-PCR)

The mRNA levels of POMT1, POMT1, POMGnT1, LARGE1, LARGE2, fukutin, and FKR1 were assessed by semiquantitative RT-PCR as described previously (Kunz *et al.*, 2006). Briefly, total RNA was isolated from HEK293T cells by using TRI Reagent (Invitrogen). Before the RT, contaminant DNA was removed by using the DNA-free kit (Ambion, Austin, TX). RT reaction was performed with 5  $\mu$ g of RNA by using SuperScript II and random hexamer primers (both from Invitrogen). PCR was done by using *Taq* polymerase by using the specific primer sets displayed in Supplemental Table S1. The mRNA of the control housekeeping actin was amplified as described previously (Sanchez *et al.*, 2005). For semiquantitative analysis, we first determined a linear range of PCR product/template by serial dilution of the RT products obtained with the control samples. To validate quantitative differences in mRNA concentration of the candidate genes infected/transfected and control samples, we performed PCR on identical RT product dilutions within the linear range of PCR product/template. PCR products were separated on agarose gels and visualized by staining with ethidium bromide. Images were acquired using an Eagle-Eye digital camera.

### Coimmunoprecipitation (coIP)

HEK293T cells were transfected with myc-tagged LARGE and flag-tagged LFGVP or flag-tagged Junin GP by using SuperFect. For cotransfection of mouse ES cells, the mouse ES Cell Nucleofector kit (Amaxa Biosystems) was used as described above with 5  $\mu$ g of expression plasmid for myc-tagged LARGE and flag-tagged GP and 5  $\times$  10<sup>6</sup> cells. After 48 h, cells were lysed in lysis buffer (1%, wt/vol, Triton X-100, 1 mM CaCl<sub>2</sub>, 1 mM MgCl<sub>2</sub>, 150 mM NaCl, 50 mM HEPES, pH 7.5, protease inhibitor complex Complete [Roche Diagnostics, Indianapolis, IN], and 1 mM phenylmethylsulfonyl fluoride) for 30 min at 4°C. CoIP was performed as described previously (Kunz *et al.*, 1996). Briefly, cleared lysates were incubated with anti-FLAG M2 affinity gel (Sigma-Aldrich) or bovine serum albumin (BSA)-conjugated Sepharose matrix as a negative control for 3 h at 4°C. The matrix was washed four times with lysis buffer, and the protein was eluted from the matrix by adding 1  $\times$  SDS-PAGE reducing buffer and boiling for 5 min at 95°C. Eluted proteins were separated by SDS-PAGE and analyzed by Western blot.

### Immunofluorescence Staining

Twenty-four hours postinfection/transfection, 10<sup>4</sup> cells were transferred to eight-well Lab-Tek chamber slides (Nalge Nunc International) precoated with poly-L-lysine. After 24 h, cells were fixed with 4% (wt/vol) paraformaldehyde, PBS for 15 min at room temperature. Primary antibodies were applied at 10  $\mu$ g/ml for 1 h at room temperature followed by fluorochrome-conjugated secondary antibodies at a dilution of 1:100 for 45 min at room temperature in the dark. For normal fluorescence microscopy, images were captured using a Zeiss Axiovert S100 microscope (Carl Zeiss, Thornwood, NY) with a 20 $\times$  objective and an AxioCam digital camera (Carl Zeiss, Thornwood, NY). For confocal laser scanning microscopy, cells were analyzed using a 1024

confocal laser microscope (Bio-Rad, Hercules, CA) an 63 $\times$  oil immersion Plan Apo, 1.4 numerical aperture objective for high resolution. Fluorescein was excited at 488 nm, rhodamine at 568 nm, and Cy5 at 647 nm all with a krypton/argon mixed gas laser recording simultaneously in three separate channels. Images were analyzed using LSM Image Examiner (Carl Zeiss), and ImageJ (<http://rsb.info.nih.gov/ij/>), and then they were assembled using Adobe Photoshop (Adobe Systems, Mountain View, CA).

### Laminin Clustering Assay

Laminin clustering assay on mouse ES cells was performed as described previously (Henry and Campbell, 1998; Henry *et al.*, 2001). Briefly, mouse DG (+/-) and DG (-/-) ES cells were plated in Permanox Lab-Teks coated with 10  $\mu$ g/ml fibronectin (Calbiochem, San Diego, CA). Cells were infected with LCMV cl-13 or Pichinde as described above for 1 h at 37°C. After washing, cells were incubated for 48 h at 37°C. Medium containing 7.5  $\mu$ g/ml (7.5 nM) mouse laminin-1 was then added to the cells, and they were incubated for 6 h. Cells were then fixed with 4% (wt/vol) paraformaldehyde, PBS for 15 min at room temperature and subjected to immunofluorescence staining for laminin and LCMV NP as described below.

## RESULTS

### Infection with LCMV Interferes with the Expression of Functional $\alpha$ -Dystroglycan in the Host Cell

To investigate the impact of arenavirus infection on the biosynthesis of  $\alpha$ -DG, we chose the immunosuppressive LCMV isolate clone-13 (cl-13) that binds  $\alpha$ -DG with high affinity and that has receptor binding characteristics similar to the human pathogenic LFV (Cao *et al.*, 1998; Kunz *et al.*, 2005b). As a control, we used the New World arenavirus Pichinde, which does not use  $\alpha$ -DG as receptor (Rojek *et al.*, 2006).

First, HEK293T cells were infected with LCMV cl-13 and Pichinde at different MOIs. After 48 h, the percentage of infected cells was determined by immunofluorescence staining for the viral GP by using mAb 83.6 to a conserved GP epitope (Weber and Buchmeier, 1988) (Figure 1A). To assess the impact of virus infection on DG biosynthesis, cells were infected for 48 h, and membrane glycoproteins were isolated using the lectin wheat germ agglutinin (WGA) (Michele *et al.*, 2002). Eluted glycoproteins were separated by reducing, denaturing SDS-PAGE. Functionally glycosylated  $\alpha$ -DG was detected by LOA (Michele *et al.*, 2002) and  $\beta$ -DG by Western blot. Infection with LCMV cl-13 but not Pichinde resulted in a dose-dependent reduction in functionally glycosylated  $\alpha$ -DG without affecting expression levels of  $\beta$ -DG (Figure 1B).

To assess changes in glycosylated  $\alpha$ -DG at the cell surface, cells infected with LCMV cl-13 or Pichinde were examined by flow cytometry using mAb IIH6 that recognizes a functional glycan epitope on  $\alpha$ -DG (Michele *et al.*, 2002). In line with the results of the LOA (Figure 1B), infection with LCMV cl-13, but not Pichinde, caused a dose-dependent reduction in the cell surface expression of functionally glycosylated  $\alpha$ -DG (Figure 1C).

To test whether the marked reduction in IIH6 staining at the cell surface was due to down-regulation of  $\alpha$ -DG protein, HEK293T and A549 human lung epithelial cells were infected with either LCMV cl-13 or Pichinde. After 48 h, cells were stained with the glycosylation sensitive anti- $\alpha$ -DG mAb IIH6 and polyclonal antibody GT20ADG that recognizes the  $\alpha$ -DG core protein independently of glycosylation (Kanagawa *et al.*, 2004). As shown in Figure 1D, infection with LCMV cl-13 resulted in a marked reduction of functionally glycosylated  $\alpha$ -DG at the surface of both cell types with only mild reduction in  $\alpha$ -DG core protein.

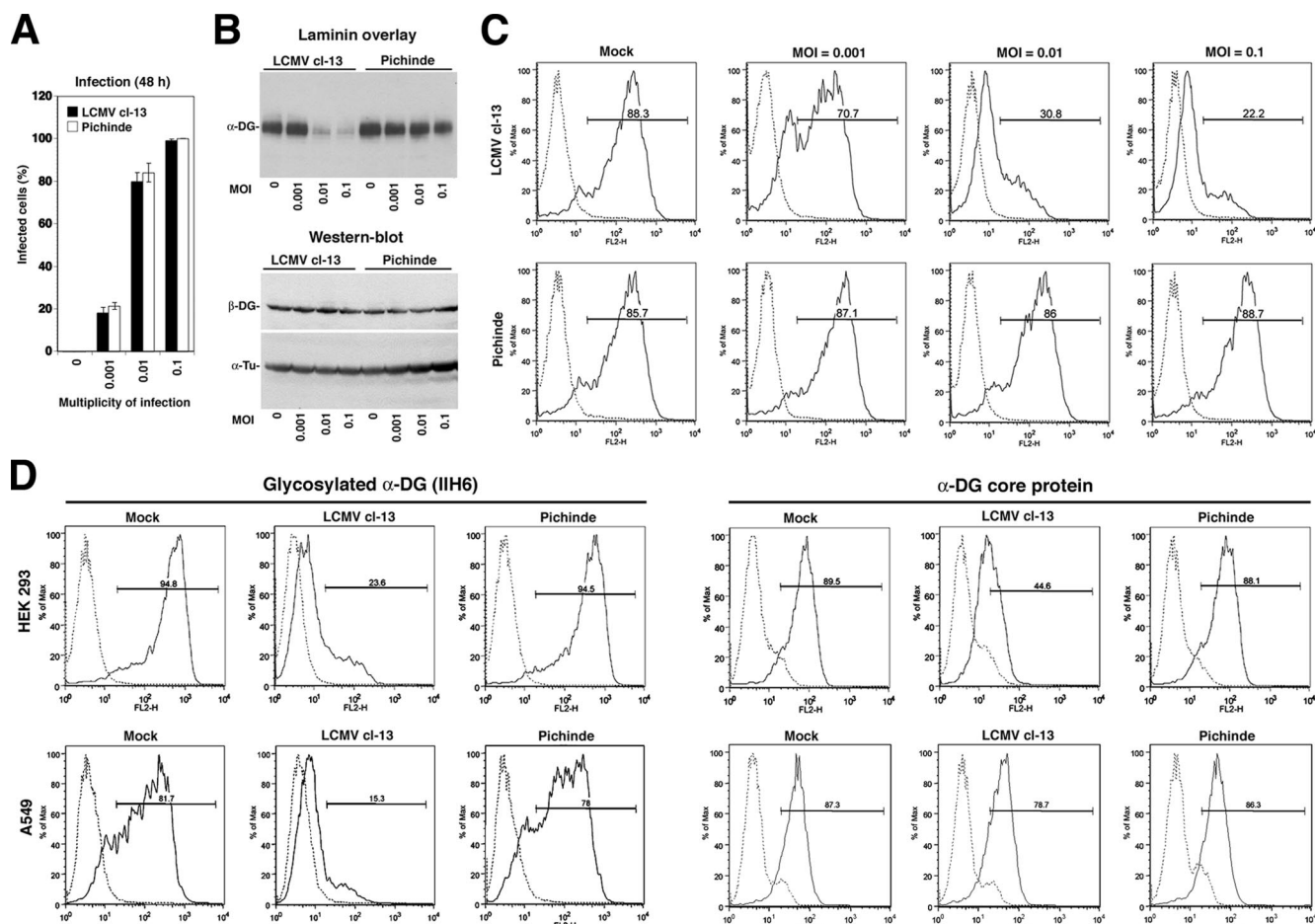


**Figure 1.** Infection with LCMV cl-13 perturbs expression of functional  $\alpha$ -DG. (A) HEK293T cells were infected with the indicated MOIs of LCMV cl-13 and Pichinde. After 48 h, cells were fixed and subjected to immunofluorescence staining by using mAb 83.6 to viral GP and an FITC-conjugated secondary antibody. In each specimen, 100 cells were counted, and GP-positive cells were scored ( $n = 3 \pm \text{SD}$ ). (B) Detection of  $\alpha$ -DG and  $\beta$ -DG in infected cells: HEK293T cells were infected with LCMV cl-13 and Pichinde at the indicated MOI. After 48 h, cells were lysed and DG isolated by WGA affinity purification. Eluted proteins were probed for functional  $\alpha$ -DG in LOA by using  $10 \mu\text{g}/\text{ml}$  mouse laminin-1 and an HRP-conjugated polyclonal anti-laminin antibody and ECL for detection.  $\beta$ -DG was detected with mAb 8D5 and an HRP-conjugated secondary antibody. For normalization  $\alpha$ -tubulin was detected in total lysates. (C and D) Detection of functionally glycosylated  $\alpha$ -DG by flow cytometry: HEK293T and A549 cells were infected with the indicated MOI of LCMV cl-13 and Pichinde (MOI = 0.1 in D). After 48 h, cell surface staining was performed with mAb IIH6 and polyclonal antibody GT20ADG to  $\alpha$ -DG core protein, combined with PE-labeled secondary antibodies. Data were acquired in a FACSCalibur flow cytometer and analyzed using FloJo software (BD Biosciences). In histograms, the  $y$ -axis represents cell numbers, and the  $x$ -axis represents PE fluorescence intensity. Solid line, primary and secondary antibody; broken line, secondary antibody only.

### Virus-induced Perturbation of $\alpha$ -DG Expression Is Mediated by the Viral GP and Depends on High Receptor Binding Affinity

To identify the viral component(s) responsible for the observed perturbation of  $\alpha$ -DG biosynthesis, we expressed the four proteins of LCMV cl-13: glycoprotein (GP), nucleoprotein (NP), polymerase (L), and matrix protein (Z) individually in HEK293T cells by using the expression vectors pC-LCMVGP (Kunz *et al.*, 2003a), pC-LCMVNP (Lee *et al.*, 2000), pC-L (Sanchez and de la Torre, 2005), and pC-ZHA (Perez *et al.*, 2003). After 48 h,  $>90\%$  of cells expressed recombinant protein. Membrane glycoproteins isolated by WGA purification were probed for functional  $\alpha$ -DG in LOA and  $\beta$ -DG in Western blot (Figure 2A). Cell surface levels of glycosylated  $\alpha$ -DG were determined by flow cytometry (Figure 2B). Expression of recombinant GP, but not NP, L, or Z protein resulted in a marked reduction in functionally glycosylated  $\alpha$ -DG without affecting  $\beta$ -DG expression (Figure 2, A and B),

indicating that GP is the viral component responsible for down-regulation of functional  $\alpha$ -DG in LCMV-infected cells.

Because the GPs of LCMV cl-13 and LFV have strikingly similar receptor binding characteristics (Kunz *et al.*, 2005b), we compared their effects on  $\alpha$ -DG expression. As a control, we included CD46EGFP, a C-terminal fusion of the cellular glycoprotein CD46 and EGFP (Kunz *et al.*, 2003b). Expression of the viral GPs but not CD46EGFP resulted in reduced cell surface expression of functional  $\alpha$ -DG and a milder reduction in  $\alpha$ -DG core protein (Figure 2C). Next, we compared the GPs of LCMV cl-13 and LFV, which bind  $\alpha$ -DG with high-affinity, with the GP of LCMV ARM53b that binds  $\alpha$ -DG with 2–3 logs less affinity (Sevilla *et al.*, 2000) and the GP of the New World arenavirus Junin that does not bind to  $\alpha$ -DG (Rojek *et al.*, 2006). All arenavirus GPs were expressed at comparable levels as assessed by cell surface staining (Figure 2D). However, only expression of the high-affinity binding GPs of LCMV cl-13 and LFV, but not the GPs of

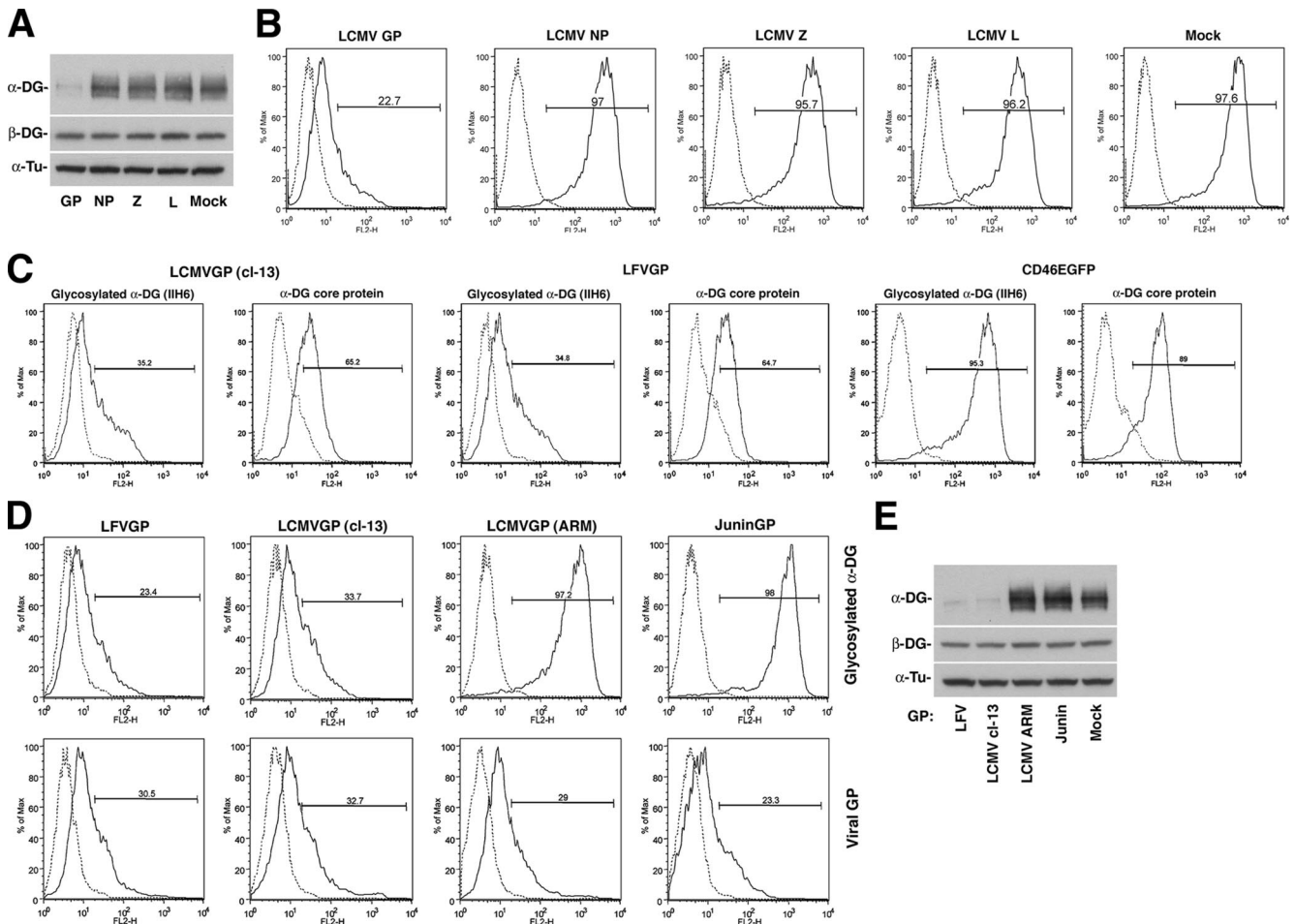


**Figure 2.** Virus-induced perturbation of  $\alpha$ -DG expression is mediated by the viral GP and depends on high receptor binding affinity. (A) Expression constructs for LCMV cl-13 GP, NP, Z, and L as well as empty vector (mock) were transfected into HEK293T cells. After 48 h, cellular glycoproteins were probed for functional  $\alpha$ -DG in LOA and for  $\beta$ -DG in Western blot as described in Figure 1B. (B) HEK293T cells transfected with LCMV cl-13 GP, NP, Z, and L, and mock-transfected controls were subjected to cell surface staining with mAb IIIH6 and flow cytometry as described in Figure 1C. The  $y$ -axis represents cell numbers, and the  $x$ -axis represents PE fluorescence intensity. Solid line, primary and secondary antibody; broken line, secondary antibody only. (C) Comparison between the effects of the GPs of LCMV cl-13 and LFV: HEK293T cells were transiently transfected with the GPs of LCMV cl-13 and LFV and the control CD46-EGFP. After 48 h, cell surface expression levels of glycosylated  $\alpha$ -DG and the  $\alpha$ -DG core protein were assessed by flow cytometry using mAb IIIH6 and antibody GT20ADG, respectively, as described in Figure 1D. (D) Interference with functional  $\alpha$ -DG expression by arenavirus GPs depends on binding affinity: The GPs of LFV, LCMV cl-13, LCMV ARM53b, and Junin virus were transiently expressed in HEK293T cells. After 48 h, cells were examined by flow cytometry using mAb IIIH6 to glycosylated  $\alpha$ -DG and mAb 83.6 to viral GPs as described in A. (E) Cells were transfected as described in D, and, after 48 h, the levels of functional  $\alpha$ -DG and  $\beta$ -DG in cell lysates were determined as described in A.

ARM53b and Junin resulted in reduced expression of functional  $\alpha$ -DG (Figure 2, D and E).

Although cell surface staining for functional  $\alpha$ -DG was markedly reduced in cells infected with LCMV cl-13 or transfected with the recombinant GPs of LFV, no detectable changes in expression of integrins  $\alpha 1$ ,  $\alpha 6$ , and  $\beta 1$ , transferrin receptor, and MHC class I heavy chain were observed (Figure 3), excluding an impact on global cell surface protein expression.

#### The Virus-induced Reduction of Functional $\alpha$ -DG Expression Is Reversible

Due to their nonlytic strategy of replication, arenaviruses can establish persistent infections in vitro and in vivo. Earlier studies demonstrated that LCMV proteins are differentially regulated during acute and persistent infec-

tion: whereas GP and NP are highly expressed in acute infection, GP is down-regulated in persistent infected cells in vitro and in vivo (Oldstone and Buchmeier, 1982). To compare virus-induced perturbation of  $\alpha$ -DG biosynthesis in acute versus persistent infection, we generated persistently infected A549 cells (Sanchez *et al.*, 2005). Briefly, A549 cells were infected with LCMV cl-13 at MOI 0.1 for 72 h, and cells subsequently passed every 2 d for 2 wk. Persistent infection was monitored by detection of viral RNA, and at 2 wk of infection, >98% of cells stained positive for NP in immunofluorescence. Examination of GP and NP expression levels by Western blot confirmed high expression of NP and GP in cells after 48 and 72 h, with a sharp decrease of GP expression in persistently infected cells (Figure 4A). Examination of  $\alpha$ -DG expression by flow cytometry revealed a marked reduction of

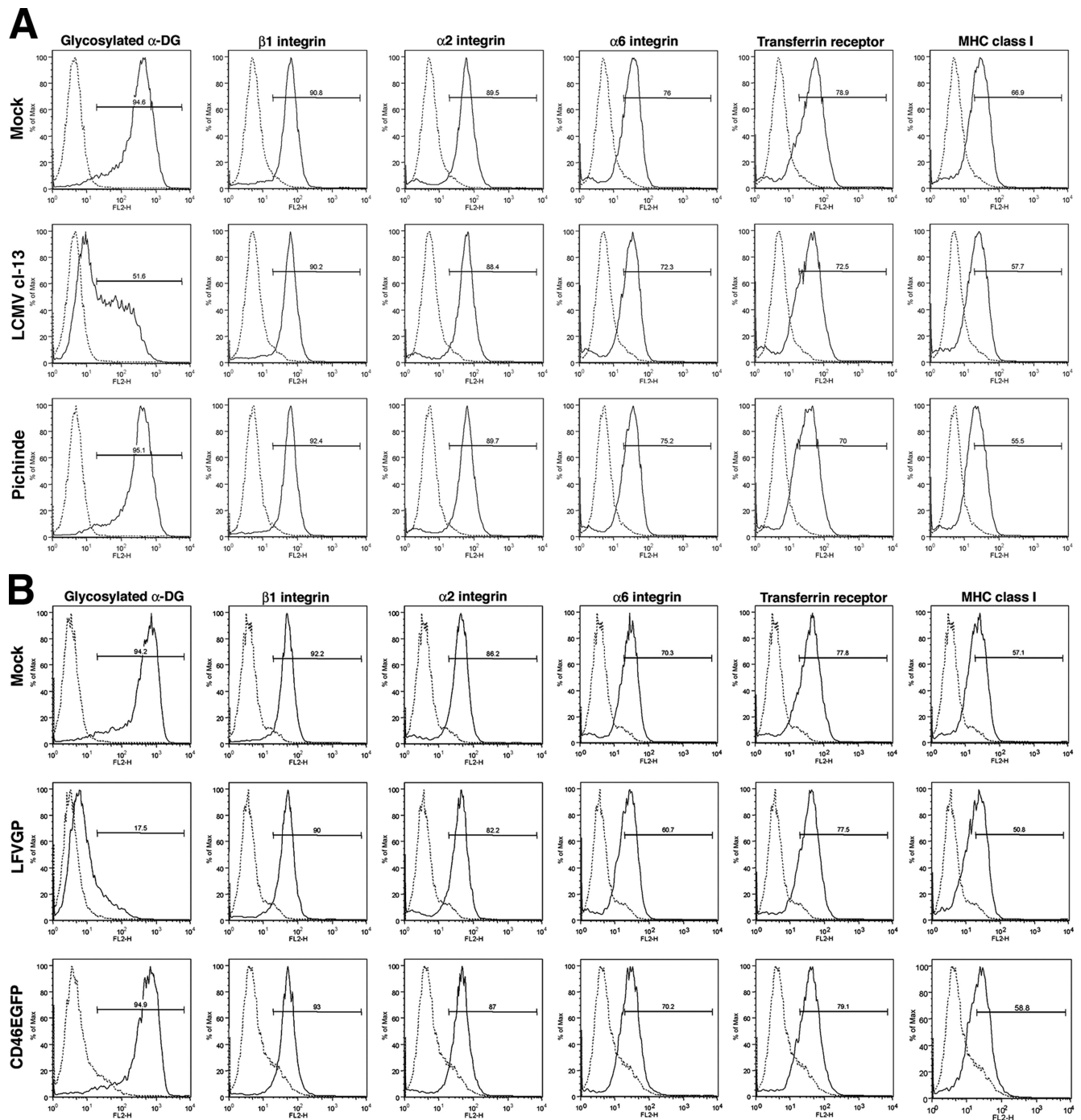


**Figure 3.** Virus infection and GP expression do not affect global cell surface expression. HEK293T cells were infected with LCMV cl-13, Pichinde (MOI = 0.1), or mock infected (A), or transfected with empty vector (Mock), LFGVP, and the control protein CD46EGFP (B), which represents a C-terminal fusion of the cellular glycoprotein CD46 with EGFP. After 48 h, the cell surface expression levels of glycosylated  $\alpha$ -DG; integrins  $\beta$ 1,  $\alpha$ 2, and  $\alpha$ 6; transferrin receptor 1; and MHC class I were examined by flow cytometry as described in *Materials and Methods*. The y-axis represents cell numbers, and the x-axis represents PE fluorescence intensity. Solid line, primary and secondary antibody; broken line, secondary antibody/isotype control.

functional  $\alpha$ -DG at 48–72 h after infection, but restoration of normal  $\alpha$ -DG glycosylation in persistently infected cells (Figure 4B). The cell surface levels of  $\alpha$ -DG core protein did not change during the time course (Figure 4B). This indicates that the virus-induced perturbation of expression of functional  $\alpha$ -DG is reversible and inversely correlates with the expression level of GP.

#### *Arenavirus Infection Does Not Affect Transcription of Glycosyltransferases Implicated in the Biosynthesis of Functional $\alpha$ -DG*

To gain insight into the molecular mechanism of virus-induced perturbation of functional  $\alpha$ -DG expression, we addressed the impact of virus infection and GP expression on transcription of known and putative glycosyltransferases

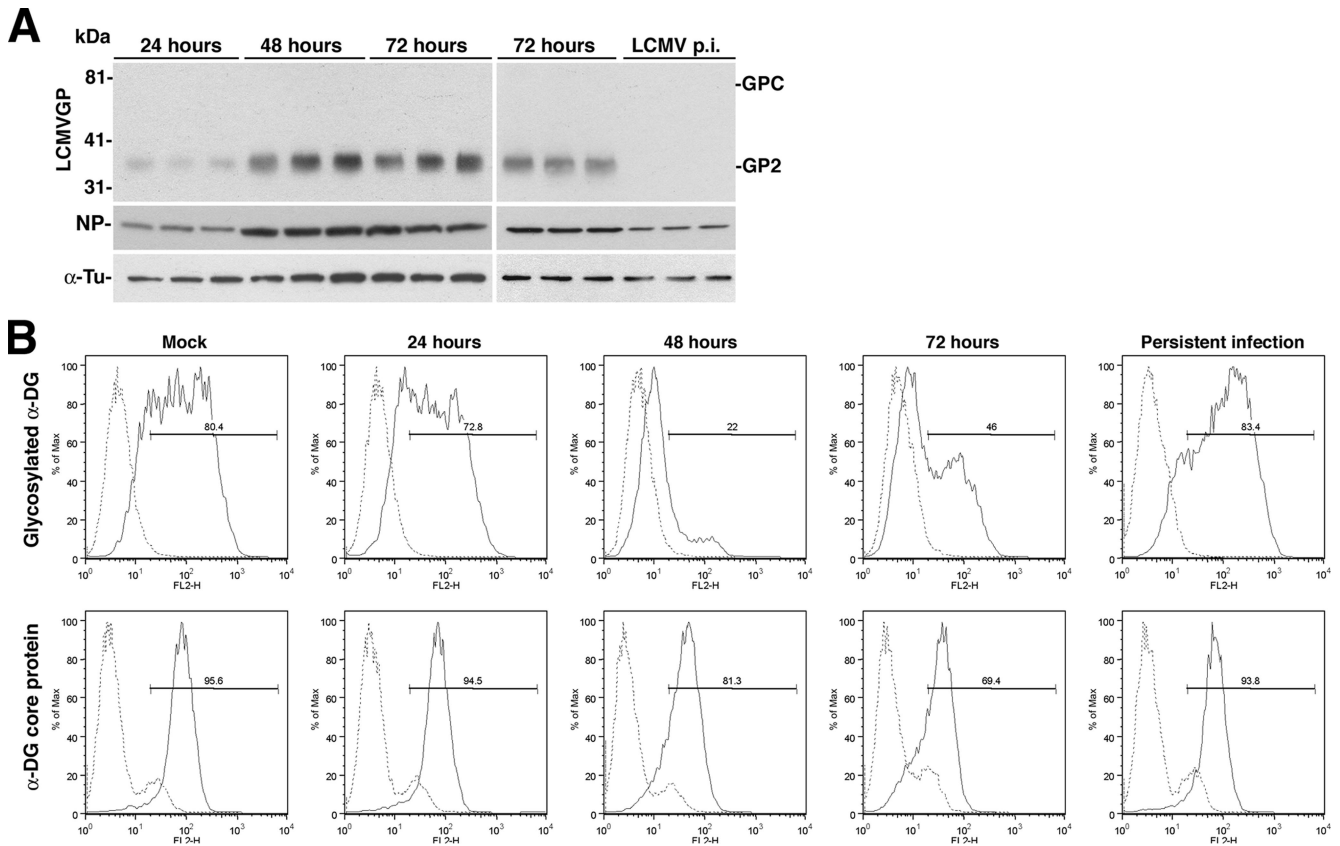


**Figure 4.** The virus-induced reduction of functional  $\alpha$ -DG expression is reversible. (A) Detection of viral protein-infected cells: triplicate samples of A549 cells infected with LCMV cl-13 for 24–72 h or persistently infected (LCMV p.i.) for 2 wk were lysed, total cell protein was extracted, and cells were probed with mAb 83.6 to GP and polyclonal antibody to NP. For normalization,  $\alpha$ -tubulin was detected. The positions of NP, the GPC, and mature GP2 are indicated. (B) Expression of functional  $\alpha$ -DG: acutely and persistently infected cells were examined for cell surface expression of glycosylated  $\alpha$ -DG and  $\alpha$ -DG core protein by flow cytometry as described in Figure 1D. The y-axis represents cell numbers, and the x-axis represents PE fluorescence intensity. Solid line, primary and secondary antibody; broken line, secondary antibody.

implicated in functional  $\alpha$ -DG glycosylation. HEK293T cells were infected with LCMV cl-13 or transfected with recombinant LCMV cl-13 and LFV GP. After 48 h, total cellular RNA was extracted, and changes in mRNA levels of POMT1, POMT2, POMGnT1, LARGE1, LARGE2, fukutin, and FKRP were addressed by semiquantitative RT-PCR (Kunz *et al.*, 2006). For each of the candidate genes, a cDNA segment of 400–500 base pairs within the open reading frame was amplified using specific sets of primers. As a control, we amplified a 400-base pair cDNA fragment of the housekeeping gene actin. The linear range of template/PCR

product ratio for each candidate gene was determined by performing PCR on serial dilutions of the corresponding RT reaction product (for details, see *Materials and Methods*). No significant changes in mRNA levels for any of the candidate genes were detected upon infection or viral GP expression (Figure 5).

**Maturation of the Viral GP Is Required for Its Ability to Interfere with the Expression of Functional  $\alpha$ -DG**

Because virus infection and GP expression did not affect the expression of genes implicated in functional  $\alpha$ -DG glycosyl-

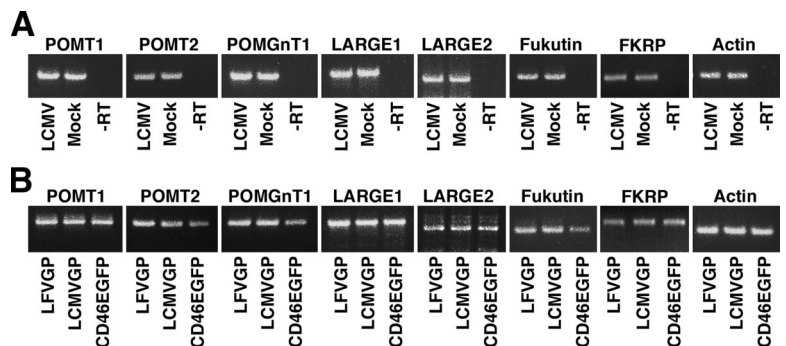


**Figure 5.** Arenavirus infection does not affect transcription of glycosyltransferases implicated in  $\alpha$ -DG glycosylation. HEK293 cells were infected either with LCMV cl-13 (MOI = 0.1), mock infected (Mock) (A), or transfected with LFVGP, LCMV cl-13 GP, or CD46EGFP (B). After 48 h, total RNA was isolated, and semiquantitative RT-PCR was performed as described in *Materials and Methods*. A control reaction without RT (–RT) is indicated.

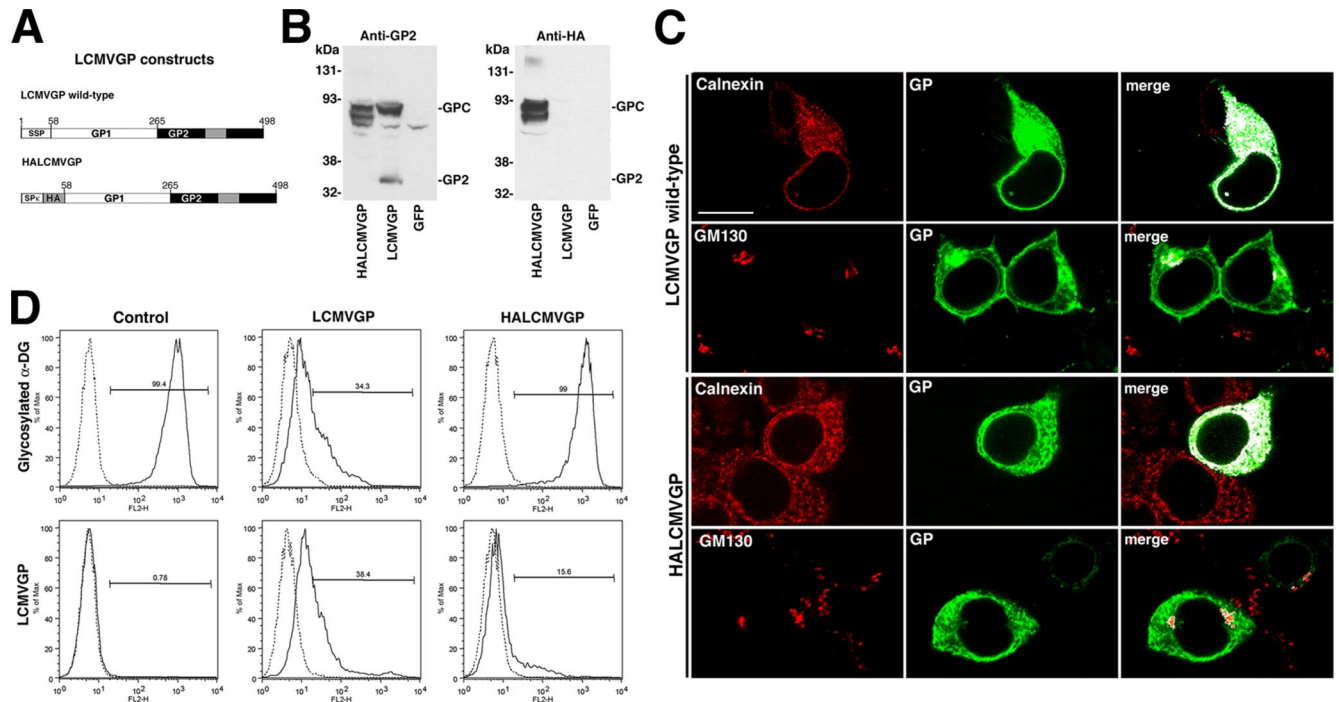


**Figure 6.** Maturation of the viral GP is required for its ability to interfere with the expression of functional  $\alpha$ -DG. (A) Schematic representation of wild-type LCMVGP and HALCMVGP. The transmembrane domain (gray box), the SSP, the Ig $\kappa$  signal peptide (SP $\kappa$ ), and the HA epitope are indicated. (B) Expression of wild-type LCMVGP and HALCMVGP: HEK293T cells were transfected with wild-type LCMVGP, HALCMVGP, or GFP. Total cell protein was extracted after 48 h and analyzed in Western blot by using mAb 83.6 (Anti-GP2) and mAb F7 to HA epitope (anti-HA). Molecular masses and the positions of the GPC and mature GP2 are indicated. (C) Cellular localization of wild-type LCMVGP and HALCMVGP: HEK293T cells were transfected with wild-type LCMVGP and HALCMVGP. After 48 h, cells were fixed, permeabilized, and stained for LCMVGP with mAb 83.6 (mouse IgG2a) to LCMV GP2 combined with mAbs to the ER marker calnexin (mouse IgG1) and the Golgi marker GM130 (mouse IgG1). Primary antibodies were detected with IgG subclass-specific secondary antibodies conjugated to FITC (green) and Rhodamine Red-X (red). Images were analyzed using LSM Image Examiner and ImageJ. Overlap of red and green signals are white in the merged image. Bar, 10  $\mu$ m. (D) Detection of LCMVGP and glycosylated  $\alpha$ -DG at the cell surface: HEK293T cells were transfected with empty vector (mock), LCMVGP, and HALCMVGP. After 48 h, cells were subjected to cell surface staining with mAb 83.6 (anti-GP) and mAb IIIH6 (glycosylated  $\alpha$ -DG) as in described in Figure 2D.

ation, we investigated posttranscriptional mechanisms. As a first step, we investigated the role of maturation of the viral GP for its ability to interfere with the expression of functional  $\alpha$ -DG. During virus infection, arenavirus GPs undergo maturation, including N-glycosylation and proteolytic cleavage by the protease S1P (Buchmeier *et al.*, 2007). Proper maturation of arenavirus GPs critically depends on their unusual stable signal peptide (SSP), which functions as a transactive maturation factor (Eichler *et al.*, 2003a,b; Froeschke *et al.*, 2003; York *et al.*, 2004; Agnihothram *et al.*, 2006). Based on previous studies, we replaced the SSP of LCMVGP by the more generic signal peptide of the immunoglobulin  $\kappa$ -light chain, followed by an influenza HA-tag, resulting in the variant HALCMVGP (Figure 6A). In HEK293T cells, HALCMVGP was expressed comparably with the wild type, but it did not undergo proper maturation, as illustrated by lack of proteolytic processing and reduced glycosylation (Figure 6B). Examination of the cellular distribution of wild-type LCMVGP and HALCMVGP by confocal microscopy revealed high concentrations of both GP variants in the ER (Figure 6C). However, in contrast to wild-type, HALCMVGP showed reduced colocalization with the Golgi marker GM130, indicating impairment in translocation from ER to Golgi. As a consequence, HALCMVGP showed markedly reduced cell surface expression as assessed by flow cytometry (Figure 6D). In contrast to wild-type LCMVGP, HALCMVGP was unable to perturb ex-

pression of functional  $\alpha$ -DG (Figure 6D), indicating that proper maturation of GP is crucial.

#### The Viral GP Associates with the DG Precursor and LARGE in an Intracellular Compartment

A crucial step in the biosynthesis of functional  $\alpha$ -DG is modification by LARGE in the Golgi (Kanagawa *et al.*, 2004). Recognition of the DG precursor by LARGE involves the N-terminal domain of  $\alpha$ -DG, which is subsequently cleaved by a furin-related protease (Kanagawa *et al.*, 2004). To test a possible interaction of the viral GP with  $\alpha$ -DG in the Golgi, we generated recombinant forms of the viral GPs, DG, and LARGE containing peptide tags for detection. For DG, we generated two mutants, one mutant with an HA-tag at the C terminus of  $\beta$ -DG (DGHA) and a variant containing an N-terminal HA-tag (HADG) (Figure 7A). HADG, DGHA, and wild-type DG showed the expected molecular masses, similar expression levels and correct processing (Figure 7B). The C-terminal tagging of  $\beta$ -DG in DGHA had no influence on expression and functional glycosylation of  $\alpha$ -DG (Supplemental Figure S1). HADG underwent proteolytic processing, resulting in removal of the N-terminal domain from the mature protein present at the cell surface (Supplemental Figure S2), as expected based on previous studies (Kanagawa *et al.*, 2004). The GPs of LCMV, LFV, and Junin virus were tagged by insertion of a flag-tag at the C terminus of GP2 (GP-flag), without adverse effects on expression and

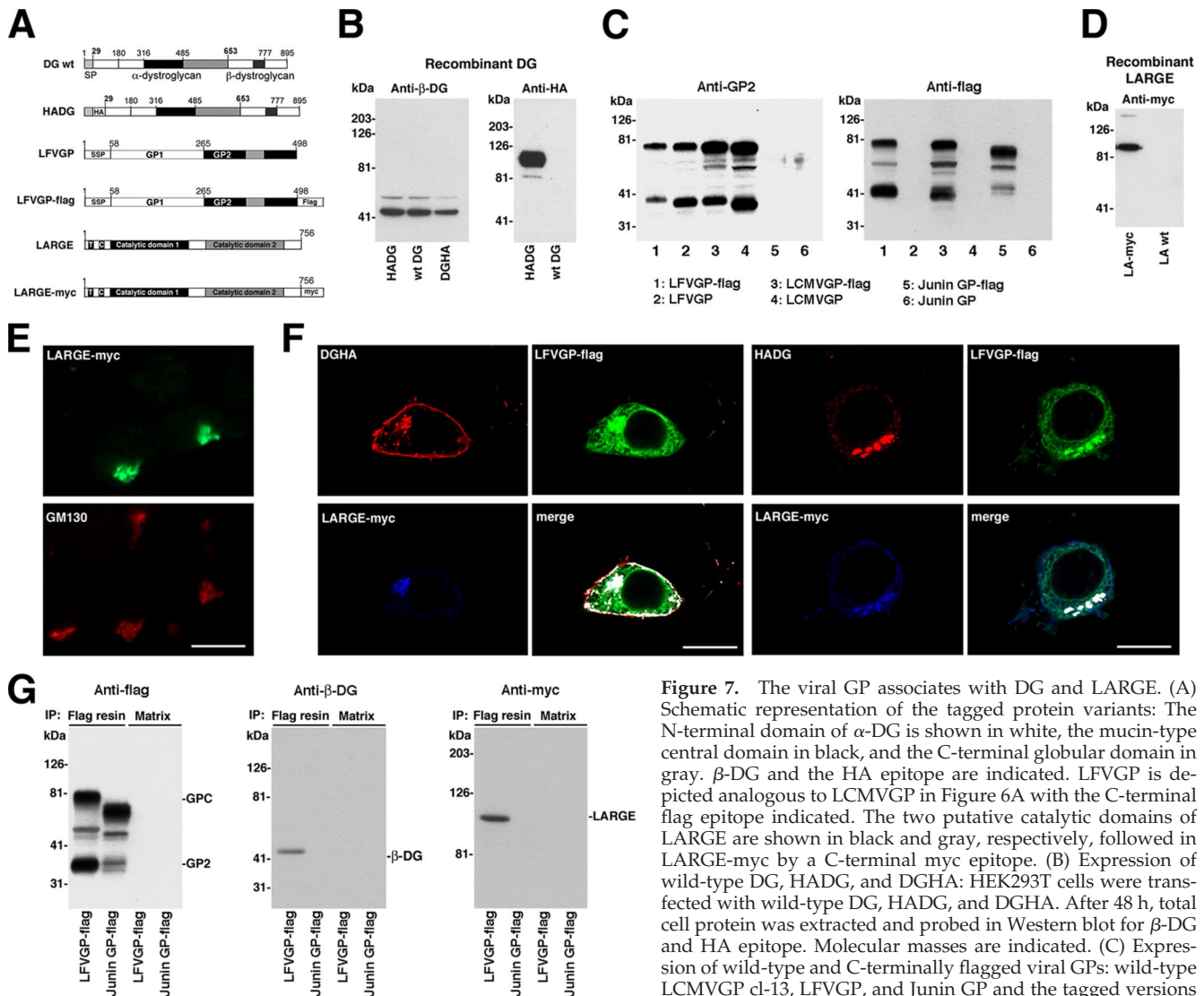


**Figure 7.** The viral GP associates with DG and LARGE. (A) Schematic representation of the tagged protein variants: The N-terminal domain of  $\alpha$ -DG is shown in white, the mucin-type central domain in black, and the C-terminal globular domain in gray.  $\beta$ -DG and the HA epitope are indicated. LfVGP is depicted analogous to LCMVGP in Figure 6A with the C-terminal flag epitope indicated. The two putative catalytic domains of LARGE are shown in black and gray, respectively, followed in LARGE-myc by a C-terminal myc epitope. (B) Expression of wild-type DG, HADG, and DGHA: HEK293T cells were transfected with wild-type DG, HADG, and DGHA. After 48 h, total cell protein was extracted and probed in Western blot for  $\beta$ -DG and HA epitope. Molecular masses are indicated. (C) Expression of wild-type and C-terminally flagged viral GPs: wild-type LCMVGP cl-13, LfVGP, and Junin GP and the tagged versions LCMVGP cl-13-flag, LfVGP-flag, Junin GP-flag, and GFP were expressed in HEK293T cells, and total cell protein was examined by Western blot by using mAb 83.6 anti-GP2 and a mAb anti-flag. Note that mAb 83.6 does not recognize Junin GP in Western blot. (D) Wild-type and C-terminally tagged LARGE (LARGE-myc) were expressed in HEK293T cells, and total cell protein was probed with an anti-myc antibody. (E) Cellular localization of LARGE-myc: LARGE-myc was transiently expressed in HEK293T cells. After 48 h, cells were fixed, permeabilized, and stained with a rabbit polyclonal antibody to myc epitope and a mouse mAb to the Golgi marker GM130. Primary antibodies were detected with secondary antibodies to mouse and rabbit IgG conjugated to FITC (green) and Rhodamine Red-X (red), respectively. Bar, 10  $\mu$ m. (F) Colocalization of DG, LfVGP, and LARGE: HEK293T cells were cotransfected with the DG variant indicated, together with LfVGP-flag and LARGE-myc. After 48 h, cells were fixed, permeabilized, and costained with mouse mAb F7 to HA epitope (DGHA, HADG), polyclonal rabbit anti-myc antibody (LARGE-myc), and a polyclonal goat anti-flag antibody (LfVGP-flag). Primary antibodies were detected with secondary antibodies anti-mouse IgG-Rhodamine Red-X (red), anti-goat IgG-FITC (green), and anti-rabbit IgG-Cy5 (blue). Confocal images were acquired as in Figure 6C. Colocalization is white in the merged images. (G) LfVGP associated with LARGE in a molecular complex: HEK293T cells were cotransfected with either LfVGP-flag or Junin GP-flag and LARGE-myc. After 48 h, cells were lysed and cleared cell lysates subjected to IP with either mAb M2 anti-FLAG conjugated to Sepharose (flag resin) or control Sepharose matrix (matrix). Immunocomplexes were separated by SDS-PAGE. Flag-tagged GPs were detected with a polyclonal rabbit antibody to flag (anti-flag).  $\beta$ -DG was detected with biotinylated mAb 8D5 (Anti- $\beta$ -DG) and streptavidin-HRP. LARGE-myc was probed with a rabbit polyclonal anti-myc antibody (anti-myc). Molecular masses and the positions of GPC, GP2,  $\beta$ -DG, and LARGE are indicated.

function of the viral GPs (Figure 7C and Supplemental Figure S3). LARGE containing a C-terminal myc tag was designed as described previously (Brockington *et al.*, 2005). LARGE-myc showed the expected molecular mass (Figure 7D) and localized in the Golgi (Figure 7E).

To study the cellular localization of the viral GP, DG, and LARGE, HEK293T cells were cotransfected with GP-flag, LARGE-myc, and either HADG or DGHA, and then they were examined by confocal microscopy. DGHA was de-

tected predominantly at the cell surface and in the Golgi (Figure 7F). In contrast, HADG was detected exclusively in intracellular compartments, because the N-terminal domain of  $\alpha$ -DG is cleaved during protein maturation (Supplemental Figure S2; Kanagawa *et al.*, 2004) (Figure 7F). In cells coexpressing DGHA, GP-flag, and LARGE-myc, all three proteins were found in the Golgi and DGHA with GP at the cell surface (Figure 7F). In cells coexpressing HADG, GP-flag, and LARGE-myc, we found intracellular colocalization

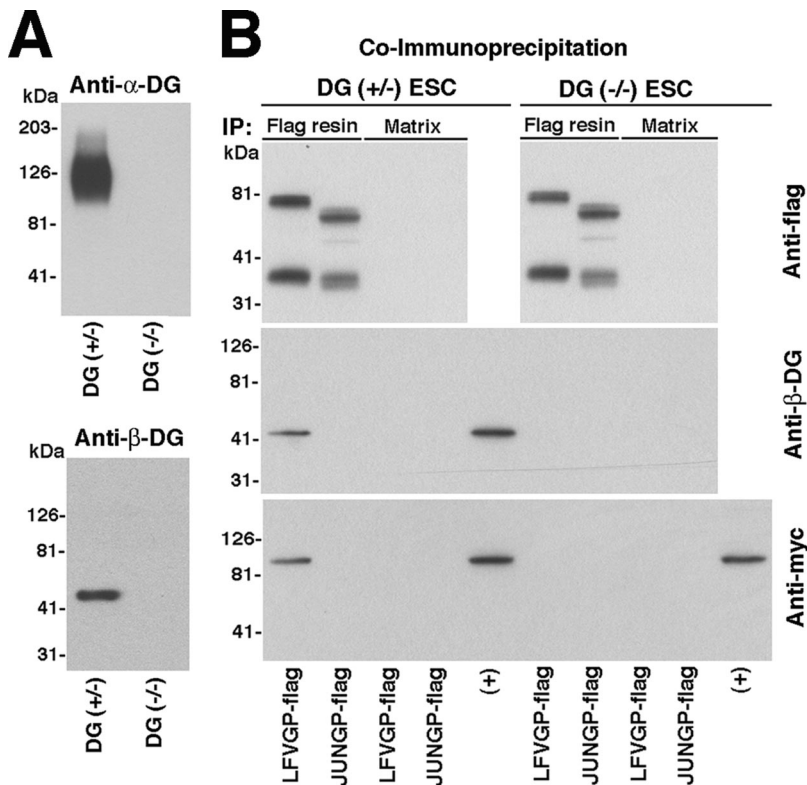


**Figure 8.** DG is required for the association of the viral GP with LARGE. (A) Absence of DG in DG (-/-) cells: Total membrane proteins extracted from DG (+/-) and DG (-/-) cells were probed with mAb IIH6 to glycosylated  $\alpha$ -DG (anti- $\alpha$ -DG) and an mAb to  $\beta$ -DG (anti- $\beta$ -DG). (B) CoIP of LfVGP with LARGE depends on DG: DG (+/-) and DG (-/-) ES cells were cotransfected with LfVGP-flag or Junin GP-flag (JUNGp-flag). After 48 h, IP with flag resin or control matrix was performed as described in Figure 7G. Immunocomplexes were probed with polyclonal antibody to flag (anti-flag), biotinylated mAb 8D5 to  $\beta$ -DG (anti- $\beta$ -DG), and polyclonal antibody to myc-tag (anti-myc). Positive control lanes (+) correspond to samples of total cell lysates to verify the presence of the indicated proteins.

of the uncleaved DG precursor HADG, the viral GP, and LARGE (Figure 7F).

To demonstrate an association between the viral GP and LARGE in a complementary approach, we used coIP. HEK293T cells were cotransfected with LfVGP-flag and LARGE-myc. As a control, we used flag-tagged GP of Junin virus, which does not bind to  $\alpha$ -DG. After 48 h, cell lysates were prepared and subjected to immunoprecipitation (IP) with mAb M2 anti-FLAG immobilized on Sepharose (flag-resin) as described previously (Sanchez and de la Torre, 2005). Pull-down with flag resin but not control matrix resulted in IP of LfVGP-flag and Junin GP-flag (Figure 7G). IP of LfVGP-flag, but not Junin GP-flag resulted in coIP of  $\beta$ -DG and LARGE-myc (Figure 7G), providing first evidence for an association of the viral GP with DG and LARGE in a molecular complex.

To gain further information about the complex formed by the viral GP, DG, and LARGE, we addressed the role of DG for the interaction between GP and LARGE. For this purpose, we performed coIP studies in mouse ES cells deficient in DG [DG (-/-)] and their hemizygous [DG (+/-)] parental line (Henry and Campbell, 1998). Although DG (+/-) ES cells express high levels of functional  $\alpha$ -DG, neither  $\alpha$ -DG nor  $\beta$ -DG expression was detected in DG (-/-) ES cells (Figure 8A). DG (+/-) and DG (-/-) ES cells were cotransfected with LfVGP-flag and LARGE-myc or the control Junin GP-flag and LARGE-myc by using nucleofection, which resulted in >80% transfection efficiency. After 48 h, cells were lysed and flag-tagged viral GPs immunoprecipitated as described above. In DG (+/-) ES cells, IP of LfVGP-flag, but not Junin GP-flag, resulted in coIP of  $\beta$ -DG and LARGE-myc (Figure 8B). In contrast, no coIP of LARGE with LfVGP was detected in lysates from DG (-/-) cells, indicating that the association of the viral GP with LARGE depends on DG.

To further investigate the role of DG in the association of GP with LARGE, we tested the activity of two well-described DG mutants: DGE (DG $\Delta$ 30-316) that lacks the binding site of LARGE and DGF (DG $\Delta$ 317-408) with a deletion of the domain modified by LARGE (Figure 9A). Consistent with previous studies (Kunz *et al.*, 2001; Kanagawa *et al.*, 2004), transfection of wild-type DG, DGE, and DGF into DG (-/-) ES cells by using AdV vectors resulted in similar expression levels, as assessed by detection of  $\beta$ -DG. However, only wild-type  $\alpha$ -DG was functionally glycosylated as shown by reaction with mAb IIH6, whereas  $\alpha$ -DG derived from DGE and DGF was not recognized. Despite differences in glycosylation, previous studies showed that DG, DGE, and DGF are expressed at similar levels at the surface of DG (-/-) ES cells (Kunz *et al.*, 2001; Kanagawa *et al.*, 2004), indicating normal transport. To test the DG variants in the context of the association of the viral GP with LARGE, DG (-/-) ES cells were conucleofected with LfVGP-flag or Junin GP-flag and LARGE-myc, followed by infection with AdV vectors expressing wild-type DG, DGE, and DGF. After 48 h, cells were lysed and coIP performed. Consistent with our results with DG (+/-) ES cells, IP of LfVGP-flag from lysates of cells expressing wild-type DG resulted in coIP of  $\beta$ -DG and LARGE (Figure 9C). In contrast, no coIP was observed in lysates of cells transfected with DGE or DGF (Figure 9C), despite similar expression levels of LfVGP-flag,  $\beta$ -DG, and LARGE-myc. This indicates that both, the LARGE binding site on DG and the region modified by LARGE are required for the formation of a complex with the viral GP and LARGE.

#### **Overexpression of LARGE Restores Functional $\alpha$ -DG in LCMV-infected Cells**

Overexpression of LARGE in cells from patients with genetic defects in  $\alpha$ -DG glycosylation can reconstitute func-

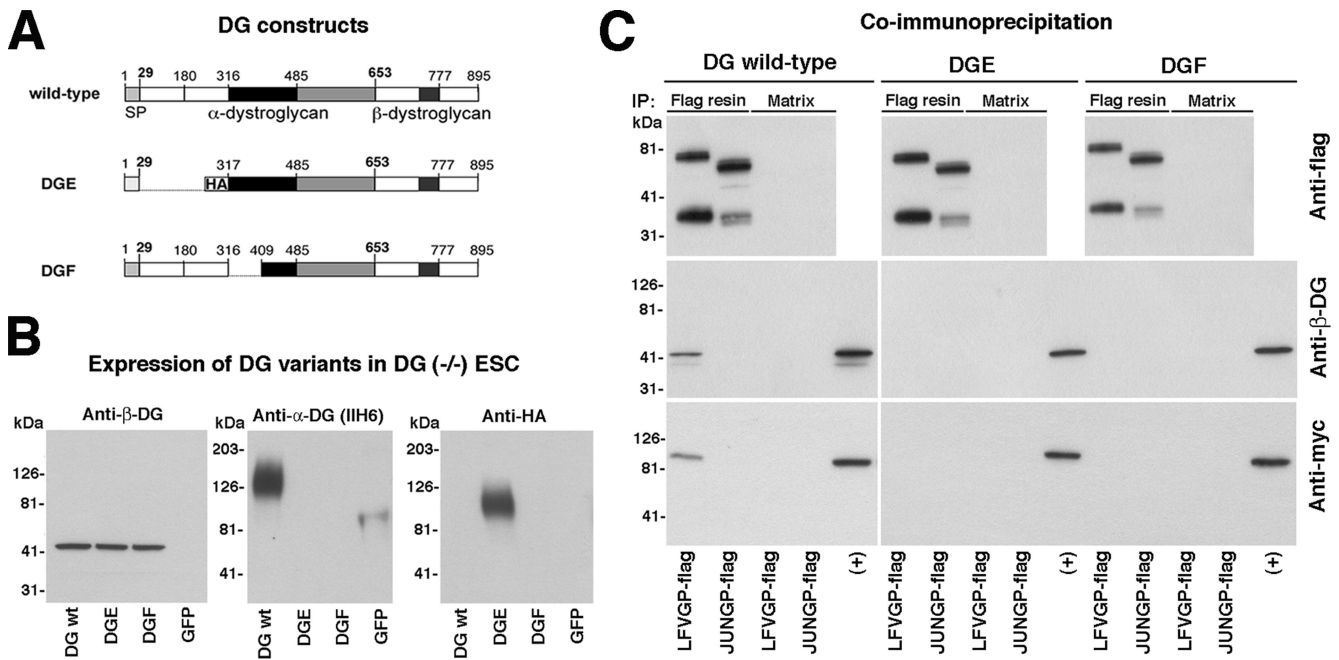


**Figure 9.** The LARGE binding site and substrate site on  $\alpha$ -DG are required for the association of LFVGP with LARGE. (A) Schematic representation of wild-type DG, DGE ( $\Delta$ 30-316), and DGF ( $\Delta$ 317-408) with DG domains depicted as in Figure 7A. (B)  $\alpha$ -DG derived from DGE and DGF lacks functional glycosylation. Wild-type DG, DGE, DGF, and GFP were expressed in DG ( $-/-$ ) ES cells by using AdV vectors. After 48 h, WGA affinity purification was performed, and eluted glycoprotein was probed in Western blot with polyclonal antibody AP83 to  $\beta$ -DG, mAb IIH6, and an anti-HA antibody. (C) CoIP of LFVGP with DG and LARGE. DG ( $-/-$ ) ES cells were cotransfected with flag-tagged GPs of LFV or Junin and LARGE-myc, followed by AdV-mediated gene transfer of wild-type DG, DGE, or DGF. After total 48 h, cell lysates were prepared, and coIP performed as described in Figure 8B. Immune complexes were separated and probed with polyclonal antibody to flag-tag (anti-flag), polyclonal antibody AP83 to  $\beta$ -DG (anti- $\beta$ -DG), and polyclonal antibody to myc tag (anti-myc). Positive control lanes (+) correspond to samples of total cell lysates to verify the presence of the indicated proteins.

tional  $\alpha$ -DG (Barresi *et al.*, 2004), indicating a pivotal role of LARGE-derived glycans for  $\alpha$ -DG function. In a similar approach, we tested whether LARGE overexpression could overcome the virus-induced perturbation in functional  $\alpha$ -DG expression. For this purpose, A549 cells were infected with LCMV cl-13, followed by infection with recombinant AdV vectors expressing either LARGE or  $\beta$ -galactosidase (LacZ). After 48 h, cells showed similar levels of LCMV NP and GP (Figure 10A), and detection of  $\beta$ -DG revealed no significant changes in DG core protein expression (Figure 10B). Overexpression of LARGE in uninfected A549 cells resulted in increased IIH6 staining at the cell surface as assessed by flow cytometry (Figure 10C), indicating hyperglycosylation of  $\alpha$ -DG. Interestingly, overexpression of LARGE, but not LacZ restored  $\alpha$ -DG glycosylation in LCMV cl-13-infected cells (Figure 10C), similar to the situation described previously with cells from patients with genetic defects in  $\alpha$ -DG glycosylation (Barresi *et al.*, 2004).

#### Virus-induced Perturbation of Functional $\alpha$ -DG Expression Prevents DG-mediated Assembly of Laminin

In the host organism, DG plays an important role in the assembly of laminin at the cell surface (Henry and Campbell, 1998; Henry *et al.*, 2001). Because binding of  $\alpha$ -DG to laminin critically depends on functional glycosylation, we studied the impact of arenavirus infection on DG-mediated laminin assembly in a well-described tissue culture model. Mouse ES cells express little if any laminin and addition of soluble laminin-1 results in the formation of characteristic laminin clusters at the cell surface (Henry and Campbell, 1998; Henry *et al.*, 2001). In contrast to wild-type cells, ES

cells deficient in DG are unable to form these clusters (Henry and Campbell, 1998), pinpointing  $\alpha$ -DG as the principal high-affinity laminin receptor. For our studies, wild-type DG (+/+ ) ES cells were plated on fibronectin, a substratum that does not involve  $\alpha$ -DG for cell adhesion. After 12 h, cells were infected with LCMV cl-13 and Pichinde virus, resulting in similar infection levels (Figure 11A). Forty-eight hours later, cell surface expression of functional  $\alpha$ -DG and the  $\alpha$ -DG core protein were assessed by flow cytometry. As observed in other cell types, infection with LCMV cl-13, but not Pichinde, resulted in significant reduction of the cell surface expression of functionally glycosylated  $\alpha$ -DG, without affecting  $\alpha$ -DG core protein (Figure 11B). To address the impact of LCMV infection on DG-mediated laminin assembly, DG (+/+) and DG ( $-/-$ ) ES cells cultured on fibronectin were infected with LCMV cl-13 or mock infected. After 48 h, the cells had formed characteristic colonies with similar gross appearance in infected and uninfected cultures. Soluble laminin-1 was added and incubated for 2 and 6 h. Cultures were fixed and stained with an antibody to laminin-1 and mAb 113 to LCMV NP. In line with previous studies (Henry and Campbell, 1998), uninfected DG (+/+) but not DG ( $-/-$ ) cells formed extensive laminin clusters at their surface (Figure 11C). In infected cultures, cells positive for LCMVNP lacked detectable laminin-clusters, whereas characteristic laminin cluster formation was observed on uninfected cells. The complementarity between viral infection and laminin cluster formation was particularly striking in ES cell colonies that were only partially infected at the time of fixation (Figure 11D). For quantification, we examined laminin clustering on equal numbers of infected (NP-

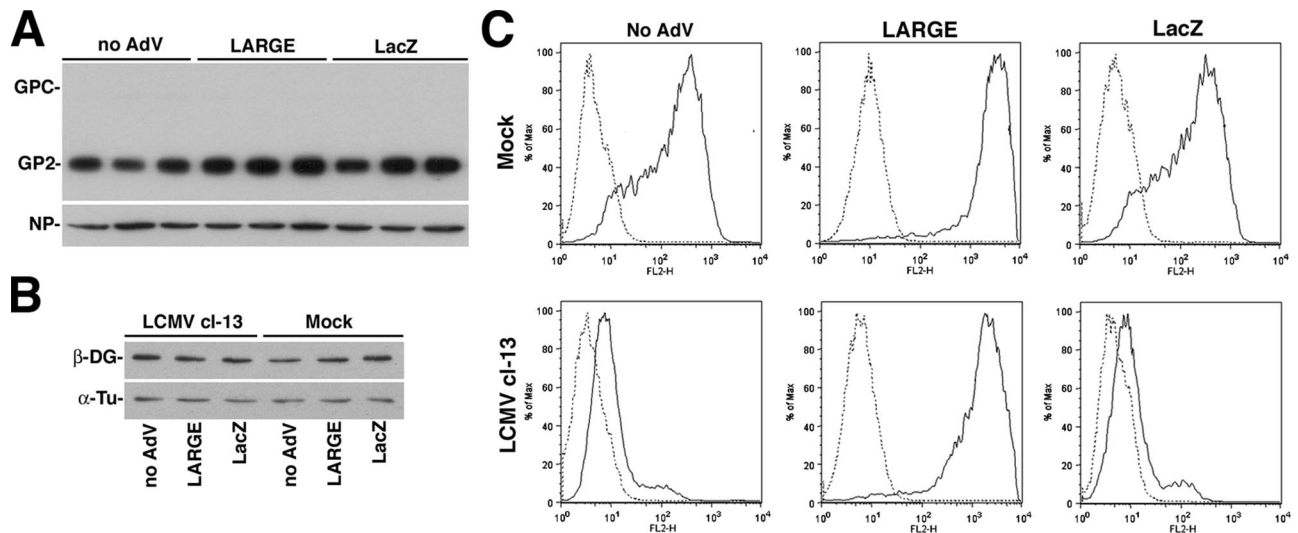


**Figure 10.** Overexpression of LARGE restores expression of functional  $\alpha$ -DG in LCMV infected cells. Detection of viral antigens (A) and  $\beta$ -DG (B) in total cell protein: Triplicate samples of A549 cells were infected with LCMV cl-13 (MOI = 0.1) or mock infected. After 4 h, cells were infected with an AdV expressing LARGE (AdV-LARGE), a control AdV-LacZ, or no AdV. Forty-eight hours after infection, total protein was extracted and probed in Western blot with specific antibodies to LCMV GP and NP as described in Figure 4A and  $\beta$ -DG and  $\alpha$ -tubulin as described in Figure 1B. The positions of GPC, mature GP2, NP, and  $\alpha$ -tubulin are indicated. (C) Overexpression of LARGE restores the expression of functional  $\alpha$ -DG in LCMV-infected cells: A549 cells were infected as described in A. After total 48 h, cell surface expression of glycosylated  $\alpha$ -DG was assessed by flow cytometry by using mAb IIH6 as in Figure 1D. In histograms, the  $y$ -axis represents cell numbers, and the  $x$ -axis represents PE fluorescence intensity. Solid line, primary and secondary antibody; broken line, secondary antibody only.

positive) and uninfected (NP-negative) ES cell colonies in infected cultures. As summarized in Figure 11E, <5% of infected ES cell colonies had detectable laminin clusters, compared with >95% of uninfected colonies. The striking inverse correlation between viral infection and laminin clusters at the cell surface in the same cultures indicated a direct effect of the virus to be responsible, rather than a general change in the culture milieu caused by virus infection. Together, the data demonstrate that virus-induced perturbation of functional  $\alpha$ -DG expression can affect DG-mediated assembly of laminin. This provides the first evidence of arenavirus-induced perturbation of the function of  $\alpha$ -DG as an ECM receptor in the host cell.

## DISCUSSION

Our present study investigated the impact of Old World arenavirus infection on expression of their cellular receptor  $\alpha$ -DG. Using the immunosuppressive LCMV cl-13 as a model, we demonstrated that virus infection caused a marked reduction in the expression of functional  $\alpha$ -DG without affecting biosynthesis of the DG core protein or global cell surface glycoprotein expression. The effect was caused by the viral GP, critically depended on high  $\alpha$ -DG binding affinity, and required proper GP maturation. An equivalent effect was observed with the GP of the human pathogenic LFV. Viral GP was found to associate with DG and LARGE in the Golgi. Overexpression of LARGE restored functional  $\alpha$ -DG expression in infected cells. We provide further first evidence that the virus-induced down-modulation of functional  $\alpha$ -DG perturbs DG-mediated cell-matrix interactions.

The interaction of a virus with its cellular receptor(s) is frequently complex. Some viruses have evolved to modulate expression and cellular trafficking of their receptors during their replication cycle as exemplified by human immunodeficiency virus type 1 (HIV-1). HIV-1 uses three of its gene

products, Vpu, Env, and Nef to down-regulate its primary receptor CD4 (Doms and Trono, 2000; Lama, 2003; Wildum *et al.*, 2006) and the principal coreceptors CCR5 (Michel *et al.*, 2005) and CXCR4 (Venzke *et al.*, 2006). Down-regulation of cellular receptors is critical for the host-virus interaction and for HIV-1 pathogenesis.

Arenaviruses use a noncytolytic strategy of multiplication, and they can cause acute and persistent infections. Infection with the immunosuppressive LCMV cl-13 induced changes in expression of functional  $\alpha$ -DG as documented by LOA and cell surface immunostaining with the glycosylation-sensitive anti- $\alpha$ -DG mAb IIH6. Both assays critically depend on a functional glycan epitope on  $\alpha$ -DG (Michele *et al.*, 2002; Kanagawa *et al.*, 2004; Kunz *et al.*, 2005a) and revealed that infection with LCMV cl-13, but not the arenavirus Pichinde, which does not use  $\alpha$ -DG as a receptor (Rojek *et al.*, 2006), markedly reduced expression of functional  $\alpha$ -DG without affecting the biosynthesis of the DG core protein.

By expressing the only four proteins of LCMV cl-13 individually in cells, we found that only the viral GP, but not NP, L, or Z was necessary and sufficient to cause the effect. Similar down-modulation of functional  $\alpha$ -DG was observed with the high-affinity binding GP of LFV, but not with the GP of LCMV ARM53b, that binds with 2–3 logs less affinity (Sevilla *et al.*, 2000) and the GP of Junin virus that does not bind to  $\alpha$ -DG (Rojek *et al.*, 2006). Because all GPs were expressed at similar levels, the data suggest that high receptor binding affinity is critical for the effect. Because LCMV and LFV recognize the glycan structures on  $\alpha$ -DG that are also implicated in binding of laminin and mAb IIH6 (Kunz *et al.*, 2005a), the observed reduction of functional  $\alpha$ -DG may be caused by either “masking” of the glycan epitopes by GP binding and/or reduced functional glycosylation. Because LOA involves denaturing conditions that destroy the active conformation of the arenavirus GP and thus dissociate the GP- $\alpha$ -DG complex, the detection of reduced levels of func-

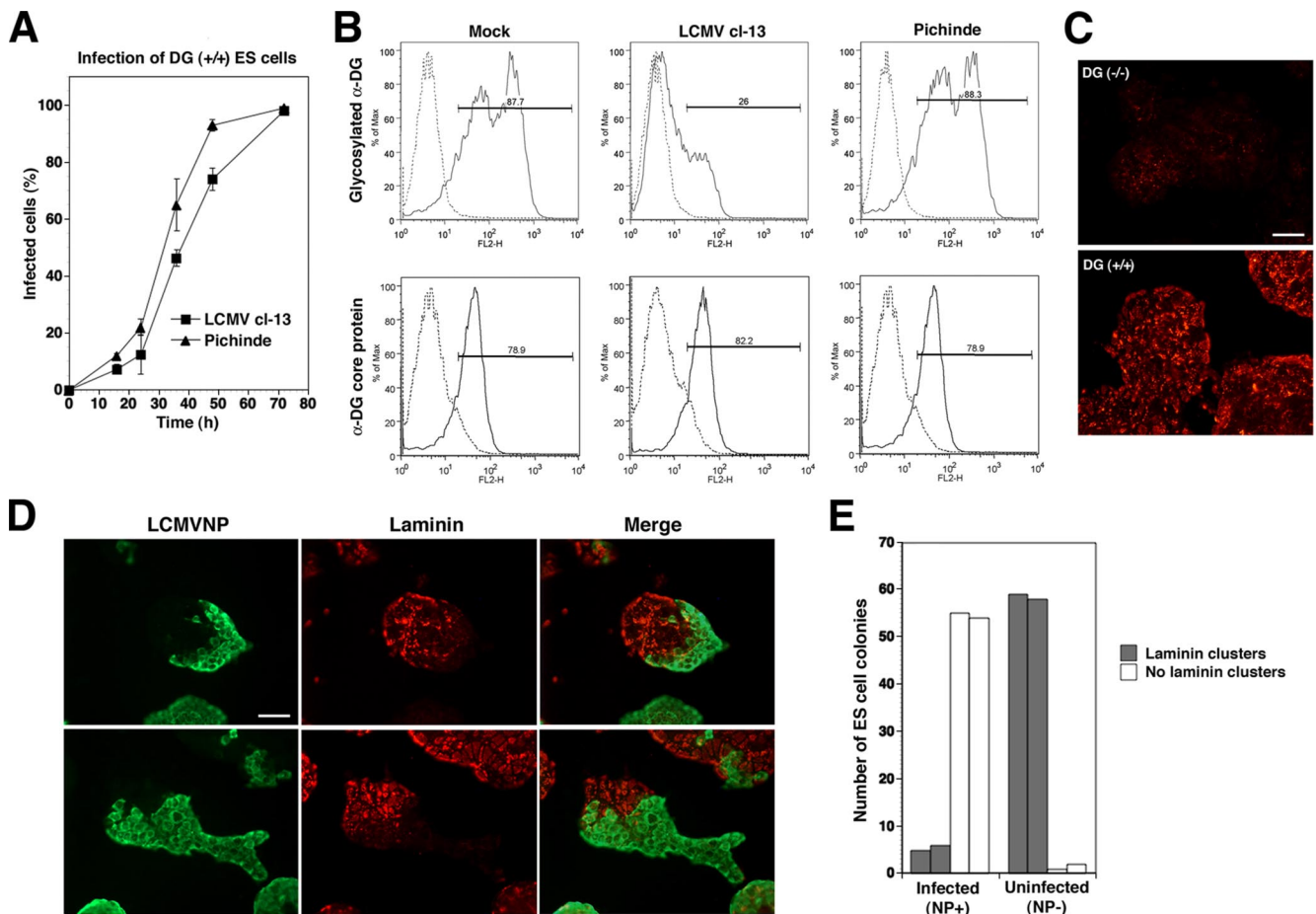


**Figure 11.** Virus-induced perturbation of functional  $\alpha$ -DG glycosylation prevents DG-mediated assembly of laminin-based ECM. (A) DG (+/+) mouse ES cells were infected with LCMV cl-13 and Pichinde at MOI = 0.3. At the time points indicated, cells were fixed, and virus infection was detected by immunostaining with mAb 83.6 as described in Figure 1A. (B) Detection of glycosylated  $\alpha$ -DG and  $\alpha$ -DG core protein on infected mouse ES cells: DG (+/+) mouse ES cells were infected with LCMV cl-13 and Pichinde at MOI = 0.3. After 48 h, cell surface expression of glycosylated  $\alpha$ -DG and  $\alpha$ -DG core protein was assessed by staining with antibodies IIH6 and GT20ADG in flow cytometry as described in Figure 1D. In histograms, the  $y$ -axis represents cell numbers, and the  $x$ -axis represents PE fluorescence intensity. Solid line, primary and secondary antibody; broken line, secondary antibody only. (C) Assembly of laminin clusters at the surface of mouse ES cells is dependent on DG: DG (+/+) and DG (-/-) mouse ES cells were cultured on fibronectin for 48 h, and soluble laminin-1 (7.5 nM) was added for 6 h. Cells were fixed, and laminin clusters were detected by immunostaining with a polyclonal anti-laminin-1 antibody and a Rhodamine Red-X-conjugated secondary antibody (bar, 50  $\mu$ m). (D) Infection of DG (+/+) ES cells with LCMV cl-13 prevents the formation of laminin clusters at the cell surface: DG (+/+) ES cells were plated on fibronectin and infected with LCMV cl-13 at MOI of 0.3. After 48 h, soluble laminin-1 was (7.5 nM) added for 2 h (top) and 6 h (bottom). Cultures were fixed, mildly permeabilized with saponin, and costained with mouse mAb 113 to LCMVNP and a rabbit polyclonal antibody to laminin-1. Primary antibodies were detected with FITC-conjugated anti-mouse IgG (green) and Rhodamine Red-X-conjugated anti-rabbit antibody (red). Colocalization in merged images is yellow. (E) Quantitative analysis: in two independent experiments, equal numbers of infected (NP+) and uninfected (NP-) ES cell colonies were counted and colonies with and without laminin clusters scored. Bar, 50  $\mu$ m.

tional  $\alpha$ -DG in this assay suggests that the viral GP can perturb  $\alpha$ -DG glycosylation. Although viral GP expression markedly reduced functional glycosylation of  $\alpha$ -DG, the biosynthesis of the core protein and global cell surface protein expression were not affected.

The biosynthesis of  $\alpha$ -DG involves a series of unusual and remarkably specific *O*-glycan modifications that are crucial for its function (Cohn, 2005; Barresi and Campbell, 2006). In the ER,  $\alpha$ -DG undergoes *O*-mannosylation by the protein-*O*-mannosyl transferases POMT1/2 (Manya *et al.*, 2004), followed by attachment of a GlcNAc residue by POMGnT1 in the Golgi (Yoshida *et al.*, 2001). A pivotal step in the biosynthesis of functional  $\alpha$ -DG is modification by LARGE. LARGE is localized in the Golgi, binds to the *N*-terminal domain of  $\alpha$ -DG, and it is implicated in the biosynthesis of

anionic sugar polymers of unknown structure, which are crucial for recognition by ECM proteins (Barresi *et al.*, 2004; Kanagawa *et al.*, 2004) and arenaviruses (Kunz *et al.*, 2005a). Two additional proteins implicated in the biosynthesis of functional DG are fukutin and FKRP, whose exact function is currently unknown. Interestingly, overexpression of LARGE can restore functional  $\alpha$ -DG in cells from patients with defects in other genes implicated in  $\alpha$ -DG glycosylation (Barresi *et al.*, 2004).

In our study, virus infection and recombinant GP expression did not affect the transcription of POMT1/2, POMGnT1, LARGE1, LARGE2, fukutin, and FKRP. This suggests that the viral GP either interferes with the transcription of a yet unknown cellular protein involved in functional  $\alpha$ -DG expression, or it acts via a posttranscrip-

tional mechanism of interference. However, we can at present not exclude possible effects of the viral GP on protein stability and/or turnover.

To address the role of viral GP maturation for its ability to perturb the functional glycosylation of  $\alpha$ -DG, we used a GP mutant lacking the endogenous SSP, which normally functions as a crucial maturation factor. Consistent with previous reports, GP lacking the SSP did not undergo proper maturation, as illustrated by defects in glycosylation, impaired ER-to-Golgi transport, absence of proteolytic processing. In contrast to wild-type GP, the SSP-deficient mutant did not perturb expression of functional  $\alpha$ -DG, indicating that proper GP maturation is crucial for its interference with  $\alpha$ -DG biosynthesis.

Considering the pivotal role of LARGE-mediated modification for expression of functional  $\alpha$ -DG, we investigated the possibility that the viral GP may associate with DG in the Golgi and interfere with modification by LARGE. Using a combination of confocal microscopy and coIP, we provide evidence that GP associates with DG that is engaged in a complex with LARGE. To address the specific role of DG in the association of the viral GP with LARGE, we performed coIP experiments in DG-deficient ES cells and their hemizygous parental line and found that DG is required for the interaction of GP with LARGE. In contrast to wild-type DG, DG variants lacking either the LARGE binding site or the domain modified by LARGE were unable to mediate an association between GP and LARGE. Although the exact composition of the complex formed by the GP, DG, and LARGE is currently unknown, our data support the hypothesis that the viral GP may bind to  $\alpha$ -DG undergoing modification by LARGE, forming a ternary complex with LARGE bound to the N-terminal domain of  $\alpha$ -DG. The precise nature of this interaction is currently under investigation. Interestingly, overexpression of LARGE restored expression of functional  $\alpha$ -DG in virus infected cells, suggesting the involvement of a similar biochemical pathway.

In the host cell,  $\alpha$ -DG serves as a high-affinity laminin receptor, and it is crucial for normal cell-ECM interactions (Barresi and Campbell, 2006). Based on the importance of  $\alpha$ -DG for normal host cell function, virus-induced perturbation of functional  $\alpha$ -DG expression is of particular interest regarding virus-induced host cell pathology. To address this issue, we used a well-characterized tissue culture model that allows the evaluation of  $\alpha$ -DG-mediated assembly of laminin. Infection of mouse ES cell cultures with LCMV cl-13 resulted in a marked reduction of functionally glycosylated  $\alpha$ -DG at the cell surface. As a consequence, infected cells failed to bind soluble laminin and to assemble characteristic laminin clusters at their surface, a phenotype similar to the one of ES cells deficient in DG (Henry and Campbell, 1998). The loss of normal  $\alpha$ -DG function seen after virus infection is also similar to the situation in cells derived from patients or animal models with genetic defects in functional glycosylation of  $\alpha$ -DG (Michele *et al.*, 2002; Barresi *et al.*, 2004; Barresi and Campbell, 2006).

The marked impact of arenavirus infection and GP expression on function of  $\alpha$ -DG as an ECM receptor has important implications for the biology of a cell during arenavirus infection. In human patients and animal models, the primary disease phenotype of congenital defects in  $\alpha$ -DG glycosylation, are muscular dystrophy and some neurodevelopmental abnormalities (Barresi and Campbell, 2006; Kanagawa and Toda, 2006). Considering the severe impact of virus infection on  $\alpha$ -DG-mediated cell-ECM interactions, the absence of overt signs of disease in persistently infected rodents in nature is interesting and best explained by the fact

that the viral GP is markedly down-regulated in persistently infected cells *in vivo* and *in vitro* (Oldstone and Buchmeier, 1982). Indeed, our present study revealed that the marked down-regulation of GP in persistently infected cells results in full recovery of functional  $\alpha$ -DG expression. Furthermore, rodents persistently infected with Old World arenaviruses show little if any viral replication in skeletal muscle (Buchmeier *et al.*, 2007). During host-virus coevolution, viruses restricted in replication in muscle cells may have been selected, because they do not affect the fitness of the host. In addition to muscle and brain,  $\alpha$ -DG is expressed abundantly on the basal side of most epithelial cells and also in some endothelial cell populations. The ability of arenavirus GPs to perturb the expression of functional  $\alpha$ -DG in the host cell makes these viruses powerful tools to investigate the largely unknown function of  $\alpha$ -DG glycosylation in cell types outside of muscle and brain. Such studies will also likely reveal novel mechanisms of virus-induced host cell pathology that occur in humans infected with the highly pathogenic LFV.

## ACKNOWLEDGMENTS

We acknowledge Drs. Juan-Carlos de la Torre (The Scripps Research Institute; TSRI) and Michael Buchmeier (TSRI) for materials, and we thank Aaron Beedle and Patricia Nienaber for preparation of antibody GT20ADG. This is publication 18755 from the Molecular and Integrative Neurosciences Department (MIND) of the Scripps Research Institute. K.P.C. is an investigator of the Howard Hughes Medical Institute. This research was supported by U.S. Public Health Service grant AI55540 (to M.B.A.O. and S.K.) and grant 1U54 AI065359 (to S.K. and J.M.R.).

## REFERENCES

- Agnihotram, S. S., York, J., and Nunberg, J. H. (2006). Role of the stable signal peptide and cytoplasmic domain of G2 in regulating intracellular transport of the Junin virus envelope glycoprotein complex. *J. Virol.* *80*, 5189–5198.
- Ahmed, R., Salmi, A., Butler, L. D., Chiller, J. M., and Oldstone, M. B. (1984). Selection of genetic variants of lymphocytic choriomeningitis virus in spleens of persistently infected mice. Role in suppression of cytotoxic T lymphocyte response and viral persistence. *J. Exp. Med.* *160*, 521–540.
- Barresi, R., and Campbell, K. P. (2006). Dystroglycan: from biosynthesis to pathogenesis of human disease. *J. Cell Sci.* *119*, 199–207.
- Barresi, R. *et al.* (2004). LARGE can functionally bypass alpha-dystroglycan glycosylation defects in distinct congenital muscular dystrophy. *Nat. Med.* *10*, 696–703.
- Brockington, M., Torelli, S., Prandini, P., Boito, C., Dolatshad, N. F., Longman, C., Brown, S. C., and Muntoni, F. (2005). Localization and functional analysis of the LARGE family of glycosyltransferases: significance for muscular dystrophy. *Hum. Mol. Genet.* *14*, 657–665.
- Buchmeier, M. J., de la Torre, J. C. and Peters, C. J. (2007). Arenaviridae: the viruses and their replication. In: *Fields Virology*, 4th ed., ed. D. L. Knipe and P. M. Howley, Philadelphia, PA: Lippincott-Raven Publishers, 1791–1828.
- Buchmeier, M. J., Lewicki, H. A., Tomori, O., and Oldstone, M. B. (1981). Monoclonal antibodies to lymphocytic choriomeningitis and Pichinde viruses: generation, characterization, and cross-reactivity with other arenaviruses. *Virology* *113*, 73–85.
- Cao, W., Henry, M. D., Borrow, P., Yamada, H., Elder, J. H., Ravkov, E. V., Nichol, S. T., Compans, R. W., Campbell, K. P., and Oldstone, M. B. (1998). Identification of alpha-dystroglycan as a receptor for lymphocytic choriomeningitis virus and Lassa fever virus. *Science* *282*, 2079–2081.
- Cohn, R. D. (2005). Dystroglycan: important player in skeletal muscle and beyond. *Neuromuscul. Disord.* *15*, 207–217.
- Coyne, C. B., and Bergelson, J. M. (2006). Virus-induced Abl and Fyn kinase signals permit coxsackievirus entry through epithelial tight junctions. *Cell* *124*:119–131.
- Doms, R. W., and Trono, D. (2000). The plasma membrane as a combat zone in the HIV battlefield. *Genes Dev.* *14*, 2677–2688.
- Durbeej, M., Henry, M. D., Ferletta, M., Campbell, K. P., and Ekblom, P. (1998). Distribution of dystroglycan in normal adult mouse tissues. *J. Histochem. Cytochem.* *46*, 449–457.

- Dutko, F. J., and Oldstone, M. B. (1983). Genomic and biological variation among commonly used lymphocytic choriomeningitis virus strains. *J. Gen. Virol.* *64*, 1689–1698.
- Eichler, R., Lenz, O., Strecker, T., Eickmann, M., Klenk, H. D., and Garten, W. (2003a). Identification of Lassa virus glycoprotein signal peptide as a transacting maturation factor. *EMBO Rep.* *4*, 1084–1088.
- Eichler, R., Lenz, O., Strecker, T., and Garten, W. (2003b). Signal peptide of Lassa virus glycoprotein GP-C exhibits an unusual length. *FEBS Lett.* *538*, 203–206.
- Ervasti, J. M., and Campbell, K. P. (1993). A role for the dystrophin-glycoprotein complex as a transmembrane linker between laminin and actin. *J. Cell Biol.* *122*, 809–823.
- Froeschke, M., Basler, M., Groettrup, M. and Dobberstein, B. (2003). Long-lived signal peptide of lymphocytic choriomeningitis virus glycoprotein pGP-C. *J. Biol. Chem.* *278*, 41914–41920.
- Geisbert, T. W., and Jahrling, P. B. (2004). Exotic emerging viral diseases: progress and challenges. *Nat. Med.* *10*, S110–S121.
- Helenius, A. (2007). Virus entry and uncoating. In: *Fields Virology*, 4th ed., ed. D. L. Knipe and P. M. Howley, Philadelphia, PA: Lippincott-Raven Publishers, 99–118.
- Henry, M. D., and Campbell, K. P. (1998). A role for dystroglycan in basement membrane assembly. *Cell* *95*, 859–870.
- Henry, M. D., Satz, J. S., Brakebusch, C., Costell, M., Gustafsson, E., Fassler, R., and Campbell, K. P. (2001). Distinct roles for dystroglycan, beta1 integrin and perlecan in cell surface laminin organization. *J. Cell Sci.* *114*, 1137–1144.
- Imperiali, M., Thoma, C., Pavoni, E., Brancaccio, A., Callewaert, N., and Oxenius, A. (2005). O-Mannosylation of alpha-dystroglycan is essential for lymphocytic choriomeningitis virus receptor function. *J. Virol.* *79*, 14297–14308.
- Kanagawa, M. *et al.* (2004). Molecular recognition by LARGE is essential for expression of functional dystroglycan. *Cell* *117*, 953–964.
- Kanagawa, M., and Toda, T. (2006). The genetic and molecular basis of muscular dystrophy: roles of cell-matrix linkage in the pathogenesis. *J. Hum. Genet.* *13*, 13.
- Kunz, S., Campbell, K. P., and Oldstone, M. B. (2003b). alpha-Dystroglycan can mediate arenavirus infection in the absence of beta-dystroglycan. *Virology* *316*, 213–220.
- Kunz, S., Edelmann, K. H., de la Torre, J.-C., Gorney, R., and Oldstone, M.B.A. (2003a). Mechanisms for lymphocytic choriomeningitis virus glycoprotein cleavage, transport, and incorporation into virions. *Virology* *314*, 168–178.
- Kunz, S., Rojek, J., Perez, M., Spiropoulou, C., and Oldstone, M. B. (2005b). Characterization of the interaction of Lassa fever virus with its cellular receptor alpha-dystroglycan. *J. Virol.* *79*, 5979–5987.
- Kunz, S., Rojek, J., Spiropoulou, C., Barresi, R., Campbell, K. P., and Oldstone, M. B. (2005a). Post-translational modification of alpha-dystroglycan, the cellular receptor for arenaviruses by the glycosyltransferase LARGE is critical for virus binding. *J. Virol.* *79*, 14282–14296.
- Kunz, S., Rojek, J. M., Roberts, A. J., McGavern, D. B., Oldstone, M. B., and de la Torre, J. C. (2006). Altered central nervous system gene expression caused by congenitally acquired persistent infection with lymphocytic choriomeningitis virus. *J. Virol.* *80*, 9082–9092.
- Kunz, S., Sevilla, N., McGavern, D. B., Campbell, K. P., and Oldstone, M. B. (2001). Molecular analysis of the interaction of LCMV with its cellular receptor alpha-dystroglycan. *J. Cell Biol.* *155*, 301–310.
- Kunz, S., Ziegler, U., Kunz, B., and Sonderegger, P. (1996). Intracellular signaling is changed after clustering of the neural cell adhesion molecules axonin-1 and NgCAM during neurite fasciculation. *J. Cell Biol.* *135*, 253–267.
- Lama, J. (2003). The physiological relevance of CD4 receptor down-modulation during HIV infection. *Curr. HIV Res.* *1*, 167–184.
- Lee, K. J., Novella, I. S., Teng, M. N., Oldstone, M. B., and de La Torre, J. C. (2000). NP and L proteins of lymphocytic choriomeningitis virus (LCMV) are sufficient for efficient transcription and replication of LCMV genomic RNA analogs. *J. Virol.* *74*, 3470–3477.
- Manya, H., Chiba, A., Yoshida, A., Wang, X., Chiba, Y., Jigami, Y., Margolis, R. U., and Endo, T. (2004). Demonstration of mammalian protein O-mannosyltransferase activity: coexpression of POMT1 and POMT2 required for enzymatic activity. *Proc. Natl. Acad. Sci. USA* *101*, 500–505.
- Marsh, M., and Helenius, A. (2006). Virus entry: open sesame. *Cell* *124*, 729–740.
- McCormick, J. B., and Fisher-Hoch, S. P. (2002). Lassa fever. *Curr. Top. Microbiol. Immunol.* *262*, 75–109.
- Michel, N., Allespach, I., Venzke, S., Fackler, O. T., and Keppler, O. T. (2005). The Nef protein of human immunodeficiency virus establishes superinfection immunity by a dual strategy to downregulate cell-surface CCR5 and CD4. *Curr. Biol.* *15*, 714–723.
- Michele, D. E. *et al.* (2002). Post-translational disruption of dystroglycan-ligand interactions in congenital muscular dystrophies. *Nature* *418*, 417–422.
- Oldstone, M. B. (2002). Biology and pathogenesis of lymphocytic choriomeningitis virus infection. *Curr. Top. Microbiol. Immunol.* *263*, 83–117.
- Oldstone, M. B., and Buchmeier, M. J. (1982). Restricted expression of viral glycoprotein in cells of persistently infected mice. *Nature* *300*, 360–362.
- Patnaik, S. K., and Stanley, P. (2005). Mouse large can modify complex N- and mucin O-glycans on alpha-dystroglycan to induce laminin binding. *J. Biol. Chem.* *280*, 20851–20859.
- Perez, M., Craven, R. C. and de la Torre, J. C. (2003). The small RING finger protein Z drives arenavirus budding: implications for antiviral strategies. *Proc. Natl. Acad. Sci. USA* *100*, 12978–12983.
- Rojek, J. M., Spiropoulou, C. F., Campbell, K. P., and Kunz, S. (2007). Old World and clade C New World arenaviruses mimic the molecular mechanism of receptor recognition used by alpha-dystroglycan's host-derived ligands. *J. Virol.* *81*, 5685–5695.
- Rojek, J. M., Spiropoulou, C. F., and Kunz, S. (2006). Characterization of the cellular receptors for the South American hemorrhagic fever viruses Junin, Guanarito, and Machupo. *Virology* *349*, 476–491.
- Sanchez, A., Pifat, D. Y., Kenyon, R. H., Peters, C. J., McCormick, J. B., and Kiley, M. P. (1989). Junin virus monoclonal antibodies: characterization and cross-reactivity with other arenaviruses. *J. Gen. Virol.* *70*, 1125–1132.
- Sanchez, A. B., and de la Torre, J. C. (2005). Genetic and biochemical evidence for an oligomeric structure of the functional L polymerase of the prototypic arenavirus lymphocytic choriomeningitis virus. *J. Virol.* *79*, 7262–7268.
- Sanchez, A. B., Perez, M., Cornu, T., and de la Torre, J. C. (2005). RNA interference-mediated virus clearance from cells both acutely and chronically infected with the prototypic arenavirus lymphocytic choriomeningitis virus. *J. Virol.* *79*, 11071–11081.
- Sevilla, N., Kunz, S., Holz, A., Lewicki, H., Homann, D., Yamada, H., Campbell, K. P., de La Torre, J. C., and Oldstone, M. B. (2000). Immunosuppression and resultant viral persistence by specific viral targeting of dendritic cells. *J. Exp. Med.* *192*, 1249–1260.
- Smith, A. E., and Helenius, A. (2004). How viruses enter animal cells. *Science* *304*, 237–242.
- Spiropoulou, C. F., Kunz, S., Rollin, P. E., Campbell, K. P., and Oldstone, M. B. (2002). New World arenavirus clade C, but not clade A and B viruses, utilizes alpha-dystroglycan as its major receptor. *J. Virol.* *76*, 5140–5146.
- Venzke, S., Michel, N., Allespach, I., Fackler, O. T., and Keppler, O. T. (2006). Expression of Nef downregulates CXCR4, the major coreceptor of human immunodeficiency virus, from the surfaces of target cells and thereby enhances resistance to superinfection. *J. Virol.* *80*, 11141–11152.
- Weber, E. L., and Buchmeier, M. J. (1988). Fine mapping of a peptide sequence containing an antigenic site conserved among arenaviruses. *Virology* *164*, 30–38.
- Wildum, S., Schindler, M., Munch, J., and Kirchhoff, F. (2006). Contribution of Vpu, Env, and Nef to CD4 down-modulation and resistance of human immunodeficiency virus type 1-infected T cells to superinfection. *J. Virol.* *80*, 8047–8059.
- York, J., Romanowski, V., Lu, M., and Nunberg, J. H. (2004). The signal peptide of the Junin arenavirus envelope glycoprotein is myristoylated and forms an essential subunit of the mature G1–G2 complex. *J. Virol.* *78*, 10783–10792.
- Yoshida, A. *et al.* (2001). Muscular dystrophy and neuronal migration disorder caused by mutations in a glycosyltransferase, POMGnT1. *Dev. Cell* *1*, 717–724.